Results

Patients' Characteristics

The patients comprised 27 women and 19 men, with a median age of 63.5 years (range, 22–87 years). Malignant diseases were diagnosed in 26 (56.5%) patients, including pancreatic cancer in 19, a malignant islet cell tumor in 4, and malignant intraductal papillary mucinous neoplasm (IPMN) in 3. The remaining 20 (43.5%) patients had benign diseases, including a benign islet cell tumor in 8 and chronic pancreatitis in 5, and benign IPMN, a solid-pseudopapillary tumor, serous cyst adenoma, mucinous cyst adenoma, schwannoma, an accessory spleen, and a pancreatic cyst in 1 patient each. The pancreatic texture at the stump of pancreatic remnant was soft and the main pancreatic duct was not dilated in all except one patient.

Morbidity Associated with Distal Pancreatectomy

A collective total of 20 postoperative complications developed in 13 (28.3%) of the 46 patients (Table 2). There were no operative or hospital deaths, nor were there any cases of intraperitoneal fluid collection or abscess. Postoperative pancreatic fistula grade B, which requires a change in management or adjustment in the clinical pathway, was observed in all patients with postoperative complications. Postoperative pancreatic fistula grade C, in which a major change in clinical management or deviation from the normal clinical pathway occurs, was not observed.

Correlations Between E-PASS Scores and Postoperative Complications

Postoperative complications were correlated significantly with performance status, ASA classification, and blood loss, but not with the other variables (Table 3). The E-PASS scores, particularly PRS and CRS, were significantly higher in patients with postoperative complications than in those without complication (Fig. 1).

Table 2. Postoperative complications

Complications	*n*
Pancreatic fistula (ISGPF grade B)	13
Delayed gastric emptying	1
Intra-abdominal bleeding	1
Cerebral hemorrhage	1
Pneumonia	1
Pleural effusion	1
Sepsis	1
Duodenal ulcer	1
Total	20

Table 3. E-PASS variables and postoperative complications

Variable	Complication			*P* value
	Total ($n = 46$)	Presence ($n = 13$)	Absence ($n = 33$)	
Mean age (years)	63.5 ± 13.4	65.1 ± 12.5	62.9 ± 13.9	NS
Severe heart-disease				NS
Presence	0	0	0	
Absence	46	13	33	
Severe pulmonary disease				NS
Presence	2	1	1	
Absence	44	12	32	
Diabetes mellitus				NS
Presence	11	4	7	
Absence	33	8	26	
Performance status				0.029
0	27	3	24	
1	13	6	7	
2	6	4	2	
ASA classification				0.023
1	15	2	13	
2	25	6	19	
3	6	5	1	
Blood loss (ml)	476.5 ± 602.7	982.9 ± 878.9	277.0 ± 275.6	0.001
Body weight (kg)	56.0 ± 11.5	60.6 ± 13.3	54.2 ± 10.4	NS
Operation time (min)	362.2 ± 98.7	430.2 ± 119.6	335.4 ± 75.6	NS

NS, not significant

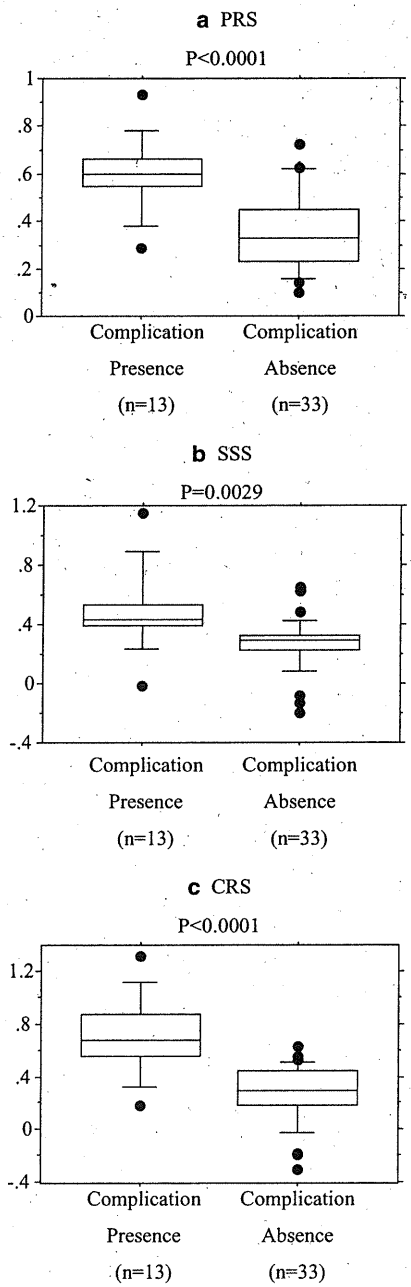

Fig. 1. Association between postoperative complications and the Estimation of Physiologic Ability and Surgical Stress (E-PASS) scores. **a** Preoperative risk score (*PRS*); **b** surgical stress score (*SSS*); **c** comprehensive risk score (*CRS*). *Boxes* show the 95% confidence intervals

The mortality rate estimated using the E-PASS scoring system was 3.4% for patients with postoperative complications. The associations between the PRS, SSS, and CRS and the complication rate are shown in Fig. 2. The complication rate tended to increase as the PRS, SSS, and CRS increased.

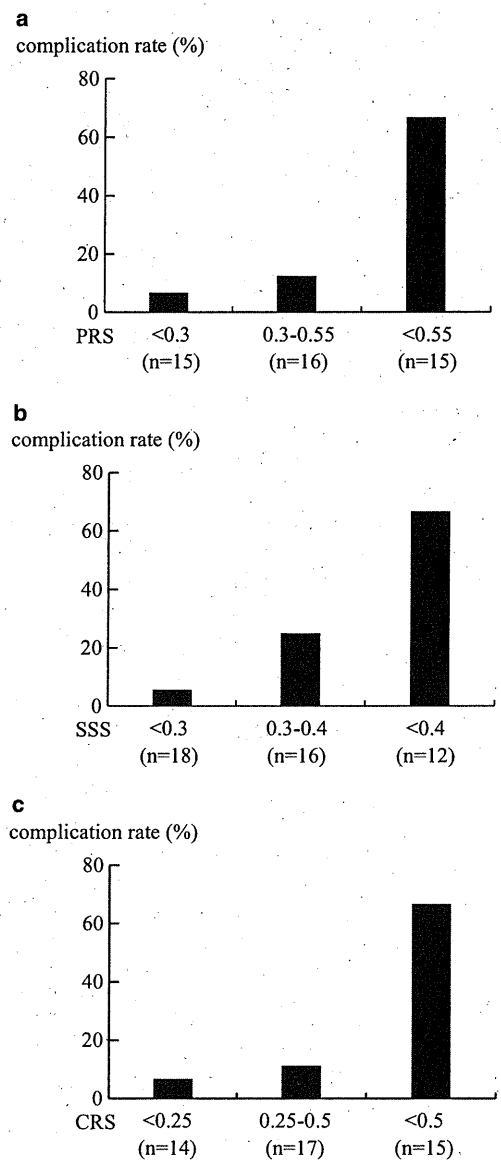

Fig. 2. Estimation of the proportion of patients with postoperative morbidity, calculated using the Estimation of Physiologic Ability and Surgical Stress (E-PASS) scores. **a** Preoperative risk score (*PRS*); **b** surgical stress score (*SSS*); **c** comprehensive risk score (*CRS*)

Receiver Operating Characteristic Analysis of the E-PASS Scores for Morbidity

The E-PASS scores showed good predictive power for morbidity associated with DP, demonstrated by the wide areas under the ROC curve in Fig. 3. The AUC was 0.84 for PRS (95% confidence interval [CI] 0.72–0.97), 0.82 for SSS (95% CI 0.67–0.97), and 0.89 for CRS (95% CI 0.77–1.01). The ROC curves show the strong associa-

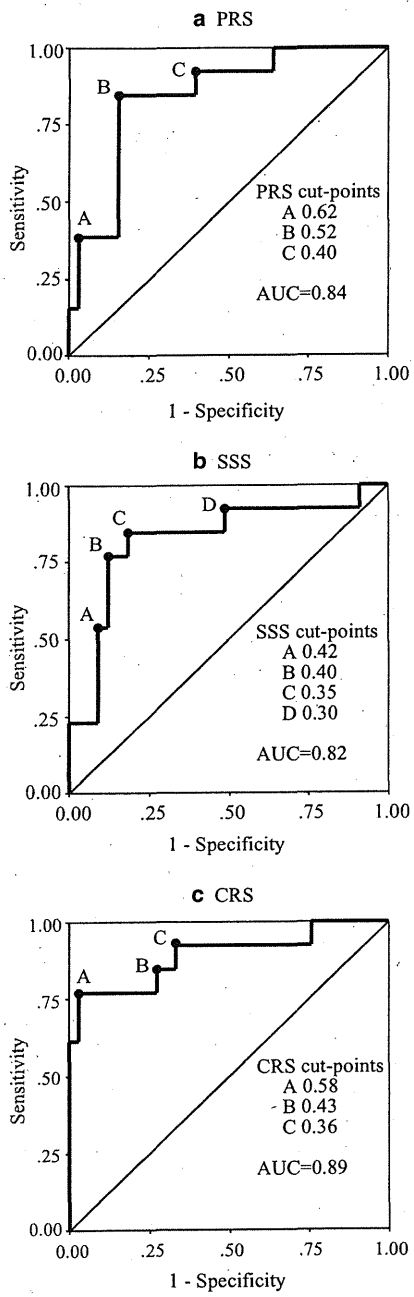

Fig. 3. Receiver operator characteristic curves for morbidity based on the Estimation of Physiologic Ability and Surgical Stress (E-PASS) scores. **a** Preoperative risk score (*PRS*); **b** surgical stress score (*SSS*); **c** comprehensive risk score (*CRS*). *AUC*, area under the curve

tion between morbidity and the PRS, SSS, and CRS individually. Fig. 3 shows various cutoff points for each graph. For CRS, a cutoff point of 0.43 would give a decision rule with sensitivity of 84.6% and specificity of 72.7% for the prediction of morbidity (Fig. 3c).

Discussion

In this series, the morbidity rate after DP was 28.3%, which is comparable with reported morbidity rates ranging from 30% to 40% in previous studies.[1–14] The E-PASS scoring system, which was developed for a general surgical audit, has been applied to various subspecialties.[18,22,24,26,27] The system is easy to use because the required information can be retrieved from preanesthetic sheets and operation notes. Kaneko et al. assessed the outcomes of laparoscopic hepatectomy (L-Hr) compared with open hepatectomy (O-Hr) for hepatocellular carcinoma (HCC), using the E-PASS scoring system.[28] They found that the SSS and CRS of the L-Hr group were significantly lower than those of the O-Hr group, although there was no difference in PRS between the two operations. In fact, the L-Hr group had a 10% complication rate, whereas the O-Hr group had a complication rate of 18%, demonstrating that the E-PASS scoring system is useful for assessing the outcome of hepatectomy for HCC.

We previously reported the good predictive power of E-PASS scores for both mortality and morbidity, as demonstrated by the large areas under the ROC curve, in patients undergoing PD.[19] In this study, we used the E-PASS scoring system to predict operative morbidity after DP and found a strong correlation between E-PASS scores and the incidence of postoperative complications. The ROC analysis in this study indicates that E-PASS scores are useful predictors of postoperative complications after DP. The E-PASS system can be used to predict operative morbidity after DP for each patient before surgery, not only by the PRS, but also the SSS and CRS, which are calculated by expected operating times and blood loss. This allows surgeons, anesthesiologists, and medical staff to evaluate high-risk patients before surgery. Although there was no mortality in this series, the E-PASS system might help surgeons consider the indications for DP in each patient and avoid performing this operation if the risks are too high. The E-PASS system can also be used to inform patients about the risks of complications before surgery. In this series, the CRS had the best predictive utility for postoperative complications. Moreover, because the SSS and CRS can be calculated immediately after DP using actual operating time and blood loss, surgeons can identify the risk of morbidity shortly after surgery, enabling the initiation of appropriate perioperative care for each patient.

The most frequent complication in this series was POPF grade B. Previous investigators have reported that pancreatic characteristics, such as soft pancreatic texture and pancreatic duct size, are predictors of POPF, including grade A.[1,6] The pancreatic texture at the stump of the pancreatic remnant was soft and the main pancreatic duct was not dilated in all but one of our patients.

Most patients undergoing DP have a soft pancreas and a normal-sized main pancreatic duct, unlike patients undergoing PD. Therefore complications after DP, including POPF, would possibly reflect the patient's own general condition and surgical stress, such as performance status, ASA classification, and blood loss, rather than pancreatic characteristics. In fact, several studies have indicated that the patient's condition, such as ASA classification, obesity, and nutritional status, and indicators of surgical stress, such as blood loss and operating time, affect the rate of postoperative complications, including POPF, after DP.[3,11,29,30] E-PASS, especially the PRS, is easy to calculate before DP. Systemic complications such as pneumonia would tend to occur in patients with high E-PASS scores, reinforcing its value before surgery. In conclusion, the E-PASS scoring system is useful for predicting operative morbidity, including POPF, in patients undergoing DP for malignant or benign pancreatic disease.

References

1. Benzoni E, Saccomano E, Zompicchiatti A, Lorenzin D, Baccarani U, Adani G, et al. The role of pancreatic leakage on rising of postoperative complications following pancreatic surgery. J Surg Res 2008;149:272–7.
2. Kooby D, Gillespie T, Bentrem D, Nakeeb A, Schmidt M, Merchant N, et al. Left-sided pancreatectomy. A multicenter comparison of laparoscopic and open approaches. Ann Surg 2008;248: 438–46.
3. Kleeff J, Diener M, Z'graggen K, Hinz U, Wagner M, Bachmann J, et al. Distal Pancreatectomy. Risk factors for surgical failure in 302 consecutive cases. Ann Surg 2007;245:573–82.
4. Mohebati A, Schwarz R. Extended left-sided pancreatectomy with spleen preservation. J Surg Oncol 2008;97:150–5.
5. Abe N, Sugiyama M, Suzuki Y, Yamaguchi T, Mori T, Atomi Y. Preoperative endoscopic pancreatic stenting: a novel prophylactic measure against pancreatic fistula after distal pancreatectomy. J Hepatobiliary Pancreat Surg 2008;15:373–6.
6. Kawai M, Tani M, Yamaue H. Transection using bipolar scissors reduces pancreatic fistula after distal pancreatectomy. J Hepatobiliary Pancreat Surg 2008;15:366–72.
7. Okano K, Kakinoki K, Yachida S, Izushi K, Wakabayashi H, Suzuki Y. A simple and safe pancreas transection using a stapling device for a distal pancreatectomy. J Hepatobiliary Pancreat Surg 2008;15:353–8.
8. Kitagawa H, Ohta T, Tani T, Tajima H, Nakagawara H, Ohnishi I, et al. Nonclosure technique with saline-coupled bipolar electrocautery in management of the cut surface after distal pancreatectomy. J Hepatobiliary Pancreat Surg 2008;15:377–83.
9. Diener M, Knaebel H, Witte S, Rossion I, Kieser M, Buchler M, et al. DISPACT trial: a randomized controlled trial to compare two different surgical techniques of DIStal PAnCreaTectomy — study rationale and design. Clinical Trials 2008;5:534–45.
10. Irani J, Ashley S, Brooks D, Osteen R, Raut C, Russell S, et al. Distal pancreatectomy is not associated with increased perioperative morbidity when performed as part of a multivisceral resection. J Gastrointest Surg 2008;12:2177–82.
11. Ferrone C, Warshaw A, Rattner D, Berger D, Zheng H, Rawal B, et al. Pancreatic fistula rates after 462 distal pancreatectomies: staplers do not decrease fistula rates. J Gastrointest Surg 2008; 12:1691–7.
12. Truty M, Sawyer M, Que F. Decreasing pancreatic leak after distal pancreatectomy: saline-coupled radiofrequency ablation in a porcine model. J Gastrointest Surg 2008;11:998–1007.
13. Koukoutsis I, Tamijmarane A, Bellagamba R, Bramhall S, Buckels J, Mirza D. The impact of splenectomy on outcomes after distal and total pancreatectomy. World J Surg Oncol 2007;5:61.
14. Carrere N, Abid S, Julio C, Bloom E, Pradere B. Spleen-preserving distal pancreatectomy with excision of splenic artery and vein: a case-matched comparison with conventional distal pancreatectomy with splenectomy. World J Surg 2007;31:375–82.
15. Sasaki A, Nitta H, Nakajima J, Obuchi T, Baba S, Wakabayashi G. Laparoscopic spleen-preserving distal pancreatectomy with conservation of the splenic artery and vein: report of three cases. Surg Today 2008;38:955–8.
16. Iso Y, Sawada T, Tagaya N, Kato M, Rokkaku K, Shimoda M, et al. Pancreatic juice leakage is a risk factor for deep mycosis after pancreatic surgery. Surg Today 2009;39:326–31.
17. Haga Y, Ikei S, Ogawa M. Estimation of physiologic ability and surgical stress (E-PASS) as a new prediction scoring system for postoperative morbidity and mortality following elective gastrointestinal surgery. Surg Today 1999;29:219–25.
18. Oka Y, Nishijima J, Oku K, Azuma T, Inada K, Miyazaki S, et al. Usefulness of an estimation of physiologic ability and surgical stress (E-PASS) scoring system to predict the incidence of postoperative complications in gastrointestinal surgery. World J Surg 2005;29:1029–33.
19. Hashimoto D, Takamori H, Sakamoto Y, Ikuta Y, Nakahara O, Furuhashi S, et al. Is Estimation of physiologic ability and surgical stress (E-PASS) able to predict operative morbidity after pancreaticoduodenectomy? J Hepatobiliary Pancreat Surg 2009; Online First. DOI: 10.1007/s00534-009-0116-4.
20. Japan Pancreas Society. General rules for the study of pancreatic cancer. 5th ed. April 2002.
21. Furue H. Criteria for the direct effect of chemotherapy against solid cancer by Japanese Society for Cancer Therapy (in Japanese). J Jpn Soc Cancer Ther 1986;21:931–42.
22. Haga Y, Wada Y, Takeuchi H, Kimura O, Furuya T, Sameshima H, et al. Estimation of physiologic ability and surgical stress (E-PASS) for a surgical audit in elective digestive surgery. Surgery 2004; 135:586–94.
23. http://ctep.cancer.gov/protocolDevelopment/electronic_applications/ctc.htm#ctc_v30
24. Baba Y, Haga Y, Hiyoshi Y, Imamura Y, Nagai Y, Yoshida N, et al. Estimation of physiologic ability and surgical stress (E-PASS system) in patients with esophageal squamous cell carcinoma undergoing resection. Esophagus 2008;5:81–6.
25. Bassi C, Dervenis C, Butturini G, Fingerhut A, Yeo C, Izbicki J, et al. Postoperative pancreatic fistula: An international study group (ISGPF) definition. Surgery 2005;138:8–13.
26. Tang T, Walsh S, Fanshawe T, Seppi V, Sadat U, Hayes P, et al. Comparison of risk-scoring methods in predicting the immediate outcome after elective open abdominal aortic aneurysm surgery. Eur J Vasc Endovasc Surg 2007;34:505–13.
27. Tang T, Walsh S, Fanshawe T, Gillard J, Sadat U, Varty K, et al. Estimation of physiologic ability and surgical stress (E-PASS) as a predictor of immediate outcome after elective abdominal aortic aneurysm surgery. Am J Surg 2007;194:176–82.
28. Kaneko H, Takagi S, Otsuka Y, Tsuchiya M, Tamura A, Katagiri T, et al. Laparoscopic liver resection of hepatocellular carcinoma. Am J Surg 2005;189:190–4.
29. Goh B, Tan Y, Chung Y, Cheow P, Ong H, Chan W, et al. Critical appraisal of 232 consecutive distal pancreatectomies with emphasis on risk factors, outcome, and management of the postoperative pancreatic fistula: a 21-year experience at a single institution. Arch Surg 2008;143:956–65.
30. Sierzega M, Niekowal B, Kulig J, Popiela T. Nutritional status affects the rate of pancreatic fistula after distal pancreatectomy: a multivariate analysis of 132 patients. J Am Coll Surg 2007; 205:52–9.

The American Journal of Surgery (2010) 199, e65–e68

The American Journal of Surgery

How I Do It

Pancreatoduodenectomy using a no-touch isolation technique

Masahiko Hirota, M.D.[a,*], Keiichiro Kanemitsu, M.D.[b], Hiroshi Takamori, M.D.[c], Akira Chikamoto, M.D.[c], Hiroshi Tanaka, M.D.[c], Hiroki Sugita, M.D.[c], Juhani Sand, M.D.[d], Isto Nordback, M.D.[d], Hideo Baba, M.D.[b]

[a]Department of Surgery, Kumamoto Regional Medical Center, 5-16-10 Honjo, Kumamoto City, Kumamoto 860–0811, Japan; [b]Department of Surgery, Saiseikai Kumamoto Hospital, Kumamoto City, Japan; [c]Department of Gastroenterological Surgery, Graduate School of Medical Sciences, Kumamoto University, Kumamoto City, Kumamoto, Japan; [d]Division of Surgery, Gastroenterology and Oncology, Tampere University, Tampere, Finland

KEYWORDS:
Pancreatoduodenectomy;
Pancreatic cancer;
Bile duct cancer;
R0 resection;
No-touch isolation technique

Abstract

BACKGROUND: Pancreatoduodenectomy is the only effective treatment for cancers of the periampullary region. Because surgeons usually grasp tumors during pancreatoduodenectomy, this procedure may increase the risk of squeezing and shedding the cancer cells into the portal vein, retroperitoneum, and/or peritoneal cavity. In an effort to overcome these problems, we have developed a surgical technique for no-touch pancreatoduodenectomy.

METHODS: From March 2005 through May 2008, 42 patients have been operated on following this technique. Resected margins were microscopically analyzed.

RESULTS: We describe a technique for pancreatoduodenectomy using a no-touch isolation technique. We resect cancers with wrapping them within Gerota's fascia and transect the retroperitoneal margin along the right surface of the superior mesenteric artery and abdominal aorta without grasping tumors.

CONCLUSIONS: No-touch pancreatoduodenectomy has many potential advantages that merit further investigation in future randomized controlled trials.

Pancreatoduodenectomy is the only effective treatment for cancers of the periampullary region. Even for patients who have undergone curative resection (R0), survival analysis has revealed a poor survival rate because of cancer recurrence, although attempts to reduce the frequency of recurrence have resulted in numerous modifications in pancreatoduodenectomy techniques.[1–5] Most postoperative recurrence is because of by hepatic metastasis, local recurrence, and peritoneal dissemination. Because surgeons usually grasp tumors during pancreatoduodenectomy, this procedure may increase the risk of squeezing and shedding the cancer cells into the portal vein, retroperitoneum, and/or peritoneal cavity. In an effort to overcome these problems, we have developed a surgical technique for improved en bloc dissection of the peripancreatic retroperitoneal margin without grasping tumors.

Surgical Technique

Transection of the pancreatic neck

One inch from the pylorus ring, the gastric antrum is divided using a linear stapler (subtotal stomach-preserving

* Corresponding author. Tel.: +81-96-363-3311; fax: +81-96-362-0222.
E-mail address: mhirota@krmc.or.jp

Manuscript received May 6, 2008; revised manuscript June 3, 2008

0002-9610/$ - see front matter © 2010 Published by Elsevier Inc.
doi:10.1016/j.amjsurg.2008.06.035

pancreatoduodenectomy), thereby exposing the neck of the pancreas. After mobilization of the gallbladder, the hepatic duct and the gastroduodenal artery are divided. The surrounding lymph nodes are dissected.

The superior mesenteric and portal veins (SMV-PV) are dissected at the inferior edge of the pancreatic neck. The right gastroepiploic vein is ligated and divided in cases of bile duct cancer or ampullary cancer. Alternatively, the accessory right colic vein and gastrocolic trunk vein are ligated and divided, and the transverse mesocolon adjacent to the pancreatic head is resected in pancreatic cancer cases. The posterior surface of the pancreatic neck is tunneled by blunt dissection. After ligating the right side of the pancreas and establishing hemostasis of the pancreatic capsule, the pancreas is transected.

Dissection of the portal venous system

The posterolateral aspect of the SMV-PV is dissected carefully and then taped. By lifting up the vascular tape, the individual pancreatic veins that drain to the SMV-PV are detected. All portal vein tributaries are ligated and divided individually until the SMV-PV is completely free from the pancreatic head. During this procedure, the pancreatic head is neither grasped nor squeezed by the surgeon. We do not yet perform the Kocher maneuver. If the tumor is approximated with or has invaded the SMV-PV, the involved SMV-PV is resected. This is usually performed with the help of an artificial bypass between the iliac vein and the intrahepatic portal vein via paraumbilical vein (or femoral vein via saphenous vein) using an antithrombogenic catheter. Thus, the involved SMV-PV is clamped and resected and then later reconstructed (see later) without extreme concern for strict time limits.[6]

Hanging up, clamping, and transection of the peripancreatic retroperitoneal margin

After division of the proximal jejunum and mobilization of the duodenojejunal junction, the proximal jejunum and the 3rd and 4th parts of the duodenum are pulled toward the right behind the superior mesenteric vessels. Next, the anterior surface of the abdominal aorta, which corresponds to the posterior plane of Gerota's fascia, around the ligament of Treiz is exposed. To permit the passage of a tape, blunt dissection of the anterior surface of the aorta is continued in a cranial direction along the right side of the superior mesenteric and the celiac trunk arteries (Figs. 1A and 1B). By lifting the tape, the plane posterior to the Gerota's fascia and anterior to the aorta can be dissected bluntly. Bleeding during this dissection was never encountered. Then, the tape is repositioned relative to the pancreatic side of the common hepatic artery and the SMV-PV cranially and relative to the pancreatic side of the left renal vein and mesocolon caudally (Fig. 1C). At this point, the tape lifts up the peripancreatic retroperitoneal margin (tissue adjacent to the SMA and

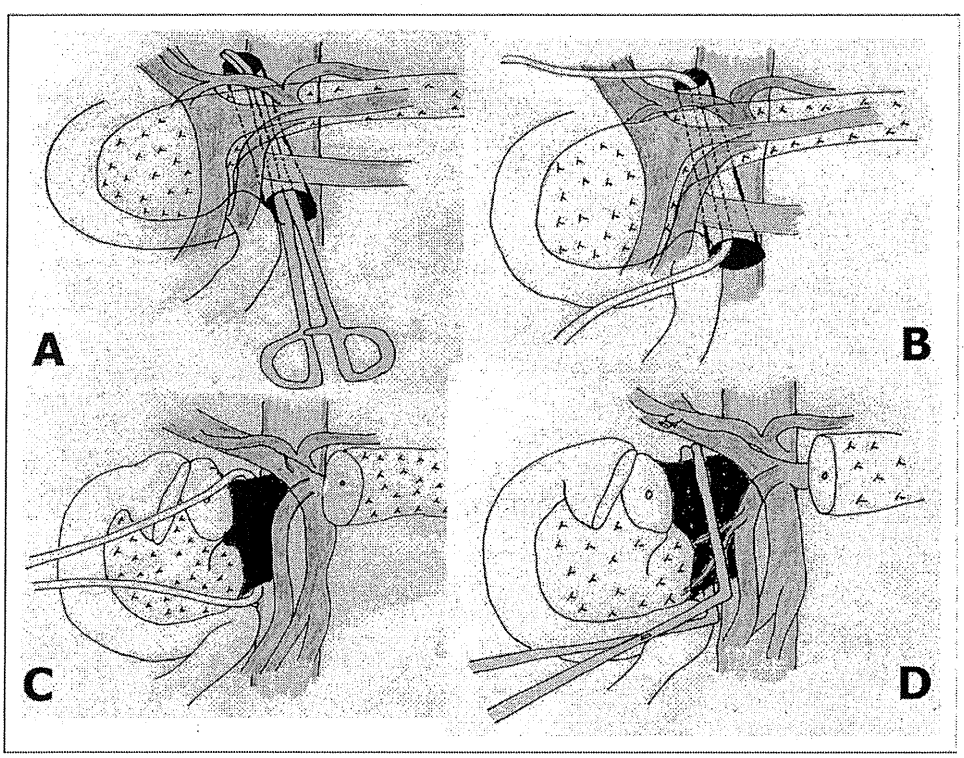

Figure 1 No-touch pancreatoduodenectomy using the hanging up and clamping technique. The anterior surface of the aorta was dissected bluntly to permit the passage of a tape (A and B). After repositioning the tape, the pancreatic side of the retroperitoneal margin is clamped (C and D). Under traction of the right-angled clamp rightward, the retroperitoneal margin is transected along with the right surface of SMA.

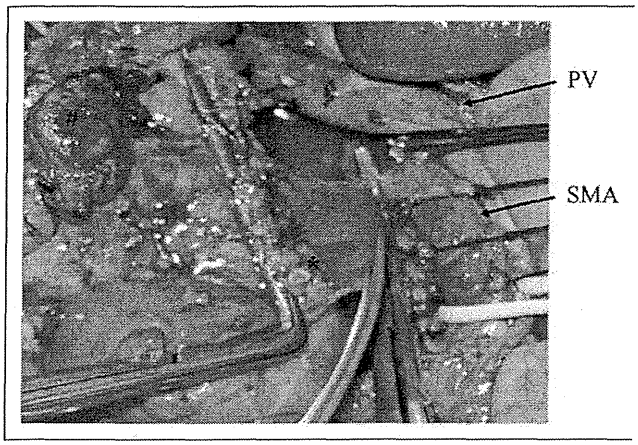

Figure 2 Transection of the retroperitoneal margin along the right surface of the superior mesenteric artery. Rightward traction of the right-angled clamp on the retroperitoneal margin and step-by-step scooping of tissue along the SMA allows identification of the inferior pancreatoduodenal artery (*). The residual side of the retroperitoneal margin is ligated to inhibit lymphatic leakage. PV, portal vein; SMA, superior mesenteric artery, #, pancreatic stump.

celiac artery), including celiac and SMA neural plexuses, lymphatic vessels, and the inferior pancreatoduodenal artery. The pancreatic side of the retroperitoneal margin is held using a long-nosed, right-angled DeBakey type aortic clamp (Figs. 1D and 2). Using rightward traction of the clamp and leftward traction of vessel tapes on the SMV-PV, the peripancreatic retroperitoneal margin is transected along the right surface of SMA, celiac artery, and the anterolateral surface of abdominal aorta. By rightward traction of the clamp, nervous and lymphatic tissue on the right and posterior aspects of the SMA is efficiently cleared (Fig. 2). Step-by-step scooping of tissue along the SMA allows identification of the inferior pancreatoduodenal artery as well as the replaced right hepatic artery. The residual side of the dissected tissue is ligated to inhibit lymphatic leakage. The tumor never serves as a "handle for retraction" of the specimen.

Reversed kocherisation

The last procedure of the resection includes reversed kocherization. The posterior plane of the Gerota's fascia is dissected medial to lateral direction, allowing exposure of the left renal vein and inferior vena cava until the "en bloc" pancreatoduodenectomy is completed. The paraaortic lymph nodes are not removed.[7] In cases of SMV-PV resection in which a shunt has been used, the vessel is now anastomosed. The retroperitoneal margin is sliced along the clamp and is submitted to frozen microscopy. Reconstruction is performed according to the surgeon's preference. After the procedure, extensive peritoneal lavage was performed with 10 L of warm saline to remove any potential dissemination of cancer cells.[8]

Hospital Outcome and Margin Status

From March 2005 through May 2008, 42 patients (17 with pancreatic ductal adenocarcinoma, 11 with extrahepatic bile duct adenocarcinoma, 6 with intraductal papillary mucinous neoplasm, 3 with ampulla of Vater cancer, 2 with nonfunctioning islet cell tumor, 1 with gastrinoma, 1 with tumor-forming chronic pancreatitis, and 1 with severe cholangitis) have been operated on following this technique. Of the 28 patients with pancreatic ductal or bile duct adenocarcinoma, 15 cases (54%) required SMV-PV resection. As for the tumor stages in these 28 patients, the final pathological stage classification (I/II/III/IVa/IVb) by the Japan Pancreas Society or Japanese Society of Biliary Surgery was 2/2/11/9/4. The International Union against Cancer stage according to pTNM pathological classification (IA/IB/IIA/IIB/III/IV) was 1/0/11/11/4/1.

Postoperative complications were as follows: 7 patients with grade B[9] pancreatic fistula (18%), 2 with intra-abdominal abscess (5%), 1 with hepatic failure (3%), 1 with liver abscess (3%), 1 with intra-abdominal bleeding from the gastric wall (3%), 1 with abdominal wall infection (3%), 1 with hyponatremia (3%), 1 with urinary infection (3%), and 1 with lymphatic leakage. The overall morbidity rate was 40%.

Resected margins were microscopically analyzed. Among the pancreatic ductal adenocarcinoma cases, 14 were R0 (microscopically margin free), 3 were R1 (microscopically margin positive), and none was R2 (macroscopically margin positive) (82%, 18%, and 0%, respectively). As for extrahepatic bile duct adenocarcinoma, 10 were R0, 1 was R1, and none was R2 (91%, 9%, and 0%, respectively). R1 resection was defined as cancer cells within 1 mm of a circumferential or transaction margin, independent of the mode of cancer spread.[10]

Two-year survival rates were both 75% for pancreatic ductal adenocarcinoma cases and extrahepatic bile duct adenocarcinoma cases with mean follow-up periods of 22.5 months and 22.9 months, respectively.

Comments

We have described a pancreatoduodenectomy technique involving a no-touch approach. We also aimed to resect cancers by wrapping them with the Gerota's fascia and to transect the peripancreatic retroperitoneal margin along the right surface of the SMA, celiac artery, and abdominal aorta. During this procedure, the pancreatic head is neither grasped nor squeezed by the surgeon.

Because our approaches also permit tumor resection without any grasping or squeezing, the technique has been named the "no-touch pancreatoduodenectomy." The no-touch isolation technique was originally adopted as a strategy to protect cancer cells from spreading because of handling malignant tumors during colon and eye cancer

surgery.[11,12] Because a pancreatic tumor is generally often grasped by the surgeon before the ligation of surrounding vessels during pancreatectomy, squeezing and handling the tumor could increase the risk of shedding cancer cells into the portal vein, retroperitoneum, and/or peritoneal cavity.[13] Hence, there is a potential for benefit using a no-touch approach in pancreatectomy as well.

A majority of studies confirm the importance of R0 resection, which may only be accomplished with techniques that position the dissecting plane further away from the tumor.[5,14–16] By rightward traction of the clamp on the peripancreatic retroperitoneal tissue, nervous and lymphatic tissue on the right and posterior aspects of the SMA can be efficiently cleared. This area is pointed out as a key area to achieve R0 resection. In the current series, comprising tumor with relatively high stages often requiring also SMV-PV resection, 82% of the pancreatic ductal and 91% of bile duct adenocarcinoma were R0.

It has been shown that pancreatic cancers with venous involvement can be resected safely, with a long-term survival similar to that observed after resection of cancers without venous involvement.[17–20] In these reports, venous resection was performed en bloc to obtain cancer-free margins. A modified technique involving posterior dissection of the pancreatic head (initially dissecting the SMA and then dividing the pancreatic neck in the final step) has been reported independently by both Pessaux et al[21] and Varty et al.[22].This modification enables a surgeon to identify signs of nonresectability as well as the presence of a replaced right hepatic artery from the SMA at an early phase of the operation. The recent advent of high-quality helical computed tomography scan images provides an alternative, preoperative method for gathering such information.

In severe acute pancreatitis, autodigestion of peripancreatic tissue by pancreatic proteases is generally provoked, whereas perirenal tissue beyond the Gerota's fascia is often protected from the autodigestion. Cancer cell invasion is also dependent on protease activity. Hence, Gerota's fascia may potentially function as a barrier against protease-mediated invasion. One of our aims was to resect cancers by wrapping them within Gerota's fascia.

In conclusion, the "no-touch" pancreatectomy procedure using the hanging and clamping maneuver for peripancreatic retroperitoneal margin resection has many theoretic advantages that merit further investigation in future randomized controlled trials.

References

1. Fortner JG, Kim DK, Cubilla A, et al. Regional pancreatectomy: en bloc pancreatic, portal vein and lymph node resection. Ann Surg 1977;186:42–50.
2. Ishikawa O. Surgical technique, curability and postoperative quality of life in an extended pancreatectomy for adenocarcinoma of the pancreas. Hepatogastroenterology 1996;43:320–5.
3. Yeo CJ, Cameron JL, Sohn TA, et al. Pancreaticoduodenectomy with or without extended retroperitoneal lymphadenectomy for periampullary adenocarcinoma: comparison of morbidity and mortality and short-term outcome. Ann Surg 1999;229:613–22.
4. Whipple AO, Parsons WB, Mullins CR. Treatment of carcinoma of the ampulla of Vater. Ann Surg 1935;102:763–79.
5. Weitz J, Kienle P, Schmidt J, et al. Portal vein resection for advanced pancreatic head cancer. J Am Coll Surg 2007;204:712–6.
6. Nakao A, Takagi H. Isolated pancreatectomy for pancreatic head carcinoma using catheter bypass of the portal vein. Hepatogastroenterology 1993;40:426–9.
7. Yeo CJ, Cameron JL, Lillemoe KD, et al. Pancreaticoduodenectomy with or without distal gastrectomy and extended retroperitoneal lymphadenectomy for periampullary carcinoma. Part 2: randomized controlled trial evaluating survival, morbidity and mortality. Ann Surg 2002;236:355–68.
8. Yamamoto K, Shimada S, Hirota M, et al. EIPL (extensive intraoperative peritoneal lavage) therapy significantly reduces peritoneal recurrence after pancreatectomy in patients with pancreatic cancer. Int J Oncol 2005;27:1321–8.
9. Bassi C, Dervenis C, Butturini G, et al. Postoperative pancreatic fistula: an international study group (ISGPF) definition. Surgery 2005; 138:8–13.
10. Verbeke CS, Leitch D, Menon KV, et al. Redefining the R1 resection in pancreatic cancer. Br J Surg 2006;93:1232–7.
11. Barnes JP. Physiologic resection of the right colon. Surg Gynecol Obstet 1952;94:722–6.
12. Turnbull RB, Jr, Kyle K, Watson FR, et al. Cancer of the colon: the influence of the no-touch isolation technique on survival rates. Ann Surg 1967;166:420–7.
13. Hirota M, Shimada S, Yamamoto K, et al. Pancreatectomy using the no-touch isolation technique followed by extensive intraoperative peritoneal lavage to prevent cancer cell dissemination: a pilot study. JOP 2005;6:143–51.
14. Hartel M, Mente M, Di SP, et al. The role of extended resection in pancreatic adenocarcinoma: is there good evidence-based justification? Pancreatology 2004;4:561–6.
15. Wagner M, Redaelli C, Lietz M, et al. Curative resection is the single most important factor determining outcome in patients with pancreatic adenocarcinoma. Br J Surg 2004;91:586–94.
16. Varadhachary GR, Tamm EP, Abbruzzese JL, et al. Borderline respectable pancreatic cancer: definitions, management, and role of preoperative therapy. Annsurg Oncol 2006;13:1035–46.
17. Bachellier Ph, Nakano H, Oussoultzoglou E, et al. Is pancreaticoduodenectomy with mesentericoportal venous resection worthwhile? Am J Surg 2001;182:120–9.
18. Kionaris LG, Schoeniger LO, Kovach S, et al. The quick, no-twist, no kink portal reconstruction. J Am Coll Surg 2003;196:490–4.
19. Leach SD, Lee JE, Charnsangavej C, et al. Survival following pancreaticoduodenectomy with resection of the superior mesenteric-portal vein confluence for adenocarcinoma of the pancreatic head. Br J Surg 1998;85:611–7.
20. Nakagohri T, Kinoshita T, Konishi M, et al. Survival benefits of portal vein resection for pancreatic cancer. Am J Surg 2003;186:149–53.
21. Pessaux P, Varma D, Arnaud JP. Pancreaticoduodenectomy: superior mesenteric artery first approach. J Gastrointest Surg 2006;10:607–11.
22. Varty PP, Yamamoto H, Farges O, et al. Early retropancreatic dissection during pancreaticoduodenectomy. Am J Surg 2005;189:488–91.

Cancer Science
The official journal of the Japanese Cancer Association JCA

The role of oxysterol binding protein-related protein 5 in pancreatic cancer

Shinji Ishikawa,[1] Youhei Nagai,[1] Toshirou Masuda,[1] Yoshikatsu Koga,[1] Tadahiko Nakamura,[1] Yu Imamura,[1] Hiroshi Takamori,[1] Masahiko Hirota,[1] Akihiro Funakosi,[2] Masakazu Fukushima[3] and Hideo Baba[1,4]

[1]Department of Gastroenterological Surgery, Graduate School of Medical Sciences, Kumamoto University, Kumamoto; [2]Department of Gastroenterology, National Kyushu Cancer Center, Minamiku, Fukuoka City; [3]Tokushima Research Center, Taiho Pharmaceutical Co. Ltd, Tokushima-shi, Tokushima, Japan

(Received September 4, 2009/Revised December 1, 2009/Accepted December 6, 2009/Online publication January 28, 2010)

The expression of oxysterol binding protein-related protein (ORP) 5 is related to invasion and a poor prognosis in pancreatic cancer patients. ORP5 induced the expression of sterol response element binding protein (SREBP) 2 and activated the downstream gene of sterol response element. ChIP using SREBP2 antibody revealed that histone deacetylase 5 (*HDAC5*) was one of the downstream genes of SREBP2. The effect of HMG-CoA reductase inhibitors (statins) were analyzed according to the expression level of *ORP5*. The invasion rate and growth was suppressed in cells that strongly expressed *ORP5* in a time- and dose-dependent manner, but had less effect in cells weakly expressing *ORP5*, suggesting that when the potential of invasion and growth relies on the cholesterol synthesis pathway, it becomes sensitive to HMG-CoA reductase inhibitor. Furthermore, HDAC inhibitor, tricostatin A, induced the expression of phosphatase and tensin homolog as well when *ORP5* was suppressed or the cells were treated with statin. Treatment with both statin and tricostatin A showed a synergistic antitumor effect in cells that highly expressed *ORP5*. Therefore, in some pancreatic cancers, continuous *ORP5* expression enhances the cholesterol synthesis pathway and this signal transduction regulates phosphatase and tensin homolog through HDAC5 expression. This is the first report to detail how the signal transduction of cholesterol synthesis is related to cancer invasion and why statins can suppress invasion and growth. (*Cancer Sci* 2010; 101: 898–905)

It is important to elucidate the mechanisms of invasion and metastasis of pancreatic cancer in order to develop an effective treatment strategy. New drugs have been developed based on the biological mechanism. Unfortunately, only a small number of patients benefit and, consequently, pancreatic cancer is still one of the most malignant tumors in the world. The mechanism of cancer development, invasion, and metastasis is complicated. Therefore, a single reagent might not be effective and combined therapy may be required. Nevertheless, signal transduction in cancer cells seems to be different in each case. For pancreatic cancer, *K-ras*, *p53*, *MEK/ERK*, and *Akt* are frequently involved and the pathway controlling the expression of these genes has been characterized.[1–4]

In previous studies, two hamster pancreatic cancer cell lines with different potential for invasion and metastasis were established. These two cell lines are from the same pancreatic ductal carcinoma induced by *N*-nitrosobis(2-oxopropyl)amine in a Syrian golden hamster.[5] The differences in mRNA expression between these two cell lines was examined using the representational difference analysis method. This identified five gene fragments that were specific in the highly invasive cell line.[6] Oxysterol binding protein-related protein (ORP) 5 was one of these genes. The suppression of *ORP5* decreased the invasion potential, and the induction of *ORP5* increased the invasion potential. Furthermore, the 1-year survival of ORP5 positive pancreatic cancer patients is 8.3 months, and 17.2 months in ORP5 negative pancreatic cancer patients.[7] *ORP5* is a member of the ORP family, which includes 12 genes.[8] There are two other reports addressing ORPs and cancer. A strong expression of *ORP8* was observed in hamster bile duct cancer in comparison to normal tissue examined by cDNA microarray.[9] *ORP8* is also strongly expressed in lung cancer tissue.[10] *ORP5* and *ORP8* belong to the same subgroup of ORPs with the same C-terminal hydrophobic segment, predicted to act as a transmembrane anchor. However, the mechanism regarding the role of ORPs in cancer is still not clear.

Signal transduction has been characterized in cholesterol synthesis.[11,12] When the cholesterol level in the cell is reduced, sterol regulatory element binding protein (SREBP) cleavage-activating protein is activated. This cleaves SREBP2, and the 58 kDa site 2 protease is transported into the nucleus, binds to sterol response element (SRE) and induces the expression of the downstream genes.[13,14] In addition to low-density lipoprotein receptor and HMG-CoA reductase, SREBP2 itself is one of these downstream genes.[15] HMG-CoA reductase is the key enzyme of cholesterol synthesis that synthesizes mevalonic acid from HMG-CoA. When the cholesterol level in the cell is on excess, oxysterol will increase. The function of oxysterol is to block the nuclear transport of site 2 protease and interrupt the cholesterol synthesis.[16] Oxysterol is related to cholesterol synthesis, and thus it is natural to consider that *ORP5* should have a role in this pathway.

This study shows that *ORP5* induces SREBP2 and alters the expression of SREBP2 downstream genes. Furthermore, this phenomenon seems to regulate the expression level of a tumor suppressor gene, thus leading to the invasion and growth of pancreatic cancer.

Materials and Methods

Cell culture. The human pancreatic cancer cell lines Capan1, Capan2, Hs700T, MiaPaCa2, and Panc1 were obtained from American Tissue Culture Collection (Rockville, MD, USA). The cells were cultured in the recommended medium supplemented with 10% FBS (Gibco-BRL, Grand Island, NY, USA) at 37°C in a humidified atmosphere of 5% CO_2 to 95% air. Various doses of histone deacetylase inhibitor, trichostatin A (TSA; Cosmo Bio, Tokyo, Japan), simvastatin, or lovastatin (both Sigma-Aldrich, St. Louis, USA) were added to the cells 24 h after seeding the cells. Total RNA or cell lysates were extracted at the optimal time.

***ORP5* suppression and induction.** siRNA for *ORP5* suppression and the construction of *ORP5* expression vector is described elsewhere.[7] RNA inhibition was carried out according to the standard protocol using Lipofectamine 2000 (Invitrogen, Carlsbad, CA, USA). Before *ORP5* or control siRNA

[4]To whom correspondence should be addressed.
E-mail: hdobaba@kumamoto-u.ac.jp

doi: 10.1111/j.1349-7006.2009.01475.x

transfection, 4×10^5 cells were plated in a six-well plate with growth medium without antibiotics. One hundred pmol of siRNA was diluted in 250 μL Opti-MEM I reduced serum medium (Gibco-BRL), and 5 μL Lipofectamine 2000 was diluted in 250 μL Opti-MEM I reduced serum medium. After a 5 min incubation at room temperature, siRNA and Lipofectamine 2000 were combined, incubated for 20 min at room temperature, added to the well, then incubated at 37°C. The transfection of expression vectors was also carried out according to the standard protocol of Lipofectamine 2000. Four micrograms of plasmid DNA was diluted in 250 μL Opti-MEM I reduced serum medium and 10 μL Lipofectamine 2000 was diluted in 250 μL Opti-MEM I reduced serum medium. After 5 min incubation at room temperature, plasmid DNA and Lipofectamine 2000 were combined, incubated for 20 min at room temperature, added to cells in a six-well plate, then incubated at 37°C. ORP5-suppressed Capan2 was designated as Capan2 – ORP5, control siRNA-transfected Capan2 as Capan2 cont.si, ORP5-induced Hs700T as Hs700T + ORP5, and LacZ-transfected Hs700T as Hs700T + LacZ.

cDNA microarray. Target DNAs made from 132 genes were immobilized on a glass plate. Each target DNA (200–600 bp) was designed based on sequence homology analysis to minimize cross-hybridization with other genes, and was practically tested by Northern blotting. The total RNA of Capan2 – ORP5, Capan2 cont.si, Hs700T + ORP5, and Hs700T + LacZ were purified using TRIzol (Invitrogen). Total RNA quality was judged from the relative intensities of the 28S and 18S ribosomal RNA bands after agarose gel electrophoresis. Purified total RNA (20 μg) was incubated at 70°C for 5 min and cooled on ice. It was reverse transcribed with a mixture of specific primers and 200 U PowerScript reverse transcriptase, and incubated at 42°C for 1.5 h. The cDNA was labeled using Cy5 (Cy5 mono-functional reactive dye; Amersham, Buckinghamshire, UK), and purified by a Nucleo Spin Extract Kit (Macherey-Nagel, Amtsgeriche, Germany). Labeled cDNA was hybridized in 6× SSC, 0.2% SDS, 0.01 mg/mL human Cot-1 DNA and 5× Denhalt's solution for 16 h at 60°C to spotted cDNA arrays. Slides were washed in 2× SSC at room temperature, then 2× SSC with 0.2% SDS at 55–65°C twice, and finally 0.05× SSC at room temperature, and scanned using a Scanner FLA-8000 (FujiFilm, Tokyo, Japan). The data were analyzed using the Array Gauge (FujiFilm). The relationship between mRNA expression of the tumor cell lines (Capan2 – ORP5 *vs* Capan2 cont.si; Hs700T + ORP5 *vs* Hs700T + LacZ) was analyzed by Pearson's correlation coefficient. The list of examined genes is shown in Table S1.

RT-PCR. Total RNA extraction was done using TRIzol and treated with DNaseI (Roche, Basel, Switzerland) to remove genomic DNA. Five micrograms of total RNA was reverse transcribed using Suprescript III (Invitrogen) according to the instruction manual. After 14–18 cycles of PCR, samples were separated on a 1.2% agarose gel and transferred to a nitrocellulose membrane (Amersham), prehybridized in PEG-SDS containing 100 μg/mL salmon sperm DNA at 65°C for 6 h. An internal probe was constructed by re-amplifying the first PCR product. A 1000× diluted first PCR product was used as a template and amplified using internal primer sets that do not include the first PCR primer sequence. Probes were gel extracted (Qiagen, Velancia, CA, USA), direct sequenced using an ABI 310 DNA sequencer (Applied Biosystems, Foster, CA, USA) for confirmation, and labeled using a psoralen–biotin non-RI labeling kit (Ambion, Austin, TX, USA). Labeled probes were added to the membrane and hybridized at 65°C overnight, washed and detected using the non-RI detection kit (Ambion), exposed on X-ray film and developed. The intensity of the band was analyzed using ImageJ software (NIH; http://rsbweb.nih.gov/ij/). The intensity of the band was compared to that of GAPDH, then the band of Capan2 cont.si was adjusted to 1 as control. The other bands were compared to the intensity of the Capan2 cont.si band and statistically analyzed using StatView computerized program (SAS Institute, Cary, NC, USA). A P-value <0.05 was considered to be significant. The primer sets for RT-PCR and for the internal probes are in Table 1.

Protein extraction and Western blot analysis. The cells were washed in PBS and lysed by radio immunoprecipitation assay buffer on ice for 15 min. The lysate was centrifuged at 3000*g* for 5 min, and the supernatant was collected. Samples were loaded on a 10% SDS-PAGE gel and transferred to a PVDF membrane (BioRad, Hurcules, CA, USA). The membranes were blocked with 5% non-fat dry milk in TBS/Tween20 (0.1%) at room temperature for 1 h, then incubated with the first antibody for 1 h at room temperature. The membranes were then washed twice, 10 min each, with TBS/Tween20, then incubated with the second antibody for 45 min at room temperature. The membranes were washed for 10 min 2x with TBS/Tween20 and for 10 min with TBS, incubated with ECL-Plus (Amersham), and exposed to an X-ray film and developed. The antibodies were β-actin (Cell Signaling Technology, Beverly, MA, USA), ORP5 (Imgenex, San Diego, CA, USA), histone deacetylase 5 (HDAC5; Calbiochem, San Diego, CA, USA), SREBP2 (Cayman Chemical, Amm Arbor, Michigan, USA), PTEN (Calbiochem), and V5 (Invitrogen).

Invasion assay. A Matrigel invasion chamber (Becton Dickinson Labware, Bedford, MA, USA) was used to examine the invasion rate. Cells were treated with TSA, simvastatin, or lovastatin for 24 h, then 5×10^4 cells were split into a 24-well Matrigel invasion chamber. The same reagent was added to the upper and lower chamber. The invading cells were counted 22 h after seeding the cells. All studies were carried out three times and examined by unpaired Student's t-test with the StatView computerized program. $P < 0.05$ was considered to be significant.

Table 1. Primers for RT-PCR and for internal probes

Gene	Forward	Reverse
ORP5	CTT, CTA, CAA, GAA, GCC, CAA, GG	GAG, ATC, TGG, TTG, ATG, CTG, GTG
HDAC5	TCG, AGA, TCC, AGA, GCA, AAC, AC	TTC, TAG, AGC, TGA, GGT, GGA, AG
SREBP2	GAG, AGC, TGT, GAA, TTC, TCC, AG	CGT, TGA, GGC, TGC, TCC, ATA, G
PTEN	ACT, TGC, AAT, CCT, CAG, TTT, GTG	TTC, CTT, GTC, ATT, ATC, TGC, ACG
GAPDH	TGA, CCA, CAG, TCC, ATG, CCA, TC	CCA, CCC, TGT, TGC, TGT, AGC, C
ORP5	TAC, ATA, GCA, GAG, CAG, GTG, TC	ATA, CAG, GAT, TCC, TTT, GCA, GTG
HDAC5	ACC, ATC, CTT, GGA, AAT, CCT, GC	TTC, TGG, AAC, TCA, GCG, AAC, AG
SREBP2	GAG, TAC, TTG, AAA, TTA, CTT, CAT, TC	TCG, CAA, TGG, CAG, AAG, GAA, CT
PTEN	TCT, GCC, AGC, TAA, AGG, TGA, AG	CTC, TAT, ACT, GCA, AAT, GCT, ATC
GAPDH	ACC, CAG, AAG, ACT, GTG, GAT, G	TCA, TAC, CAG, GAA, ATG, AGC, TTG

HDAC5, histone deacetylase 5; ORP5, oxysterol binding protein-related protein; SREBP2, sterol response element binding protein.

Growth assay and synergistic effect of statins and TSA. Cells (5×10^4) were seeded in a 12-well plate the day before examination. Various doses of TSA, simvastatin, and lovastatin were added to the cells. The medium including the reagents was changed daily. The cells were trypsinized, stained by Trypan blue and counted after 6 days. For the synergistic effect of statin and TSA, 5×10^4 cells were seeded in a 12-well plate the day before examination, 5 μM simvastatin was used for simvastatin alone, 80 ng/mL TSA was used for TSA alone, and 5 μM simvastatin and 80 ng/mL TSA was used for combination treatment. Cells were counted from days 1 to 7. The medium including the drugs was changed daily. All experiments were done in triplicate.

ChIP assay. ChIP was carried out using an Orange ChIP Kit (Daigenode, Liege Area, Belgium) according to the instruction manual. A sample containing 1×10^7 Capan2 or Hs700T cells were fixed in 1% formaldehyde for 10 min. Glycine was added to a final concentration of 125 mM. Cells were washed twice with ice-cold PBS. Cells were scraped and collected in a 15 mL tube. Samples were sonicated to 200–600 bp DNA fragments using a sonicator, centrifuged for 5 min at 12 000*g* at room temperature. The supernatant was collected as the cleared sample. One microgram of SREBP2 antibody was added to 10 μL cleared samples and rotated at 4°C overnight. Mouse IgG was used as the negative control. Beads were added to the samples and incubated at 4°C on a rotating wheel for 1 h. Beads were washed and precipitated. Ten microliters of the cleared sample was used as a positive control which corresponded to the 'input sample'. After incubating the samples for 4 h at 65°C to reverse cross-linking, the DNA was recovered by phenol–chloroform–isoamyl alcohol treatment and ethanol precipitation. Recovered DNA was resuspended in 50 μL distilled water. Thirty cycles of PCR were carried out 1 μL DNA samples and visualized on a 2% agarose gel. The primer set for each putative site was: site 1, 5′-AGC ACT GTA GCT TGC TCA TG (forward), 5′-ACC TCA GGC AGA ATG ATA CC (reverse); site 2, 5′-GCA CAA GGA TCA GAA AGT CG (forward), 5′-TTC AGG TGA GTG TCT ACT GC (reverse); and site 3, 5′-GGT CTA TCC AGT TCT GCA GA (forward), 5′-TGC CCA TCC GAG GCC ATC (reverse).

Results

***ORP5* induction and suppression.** Five human pancreatic cancer cell lines were evaluated for *ORP5* expression. The expression of *ORP5* was strong in Capan1, Capan2, and Panc1, moderate in MiaPaCa2, and very weak in Hs700T (Fig. 1A). Capan2 was selected as an *ORP5* highly expressing cell line and

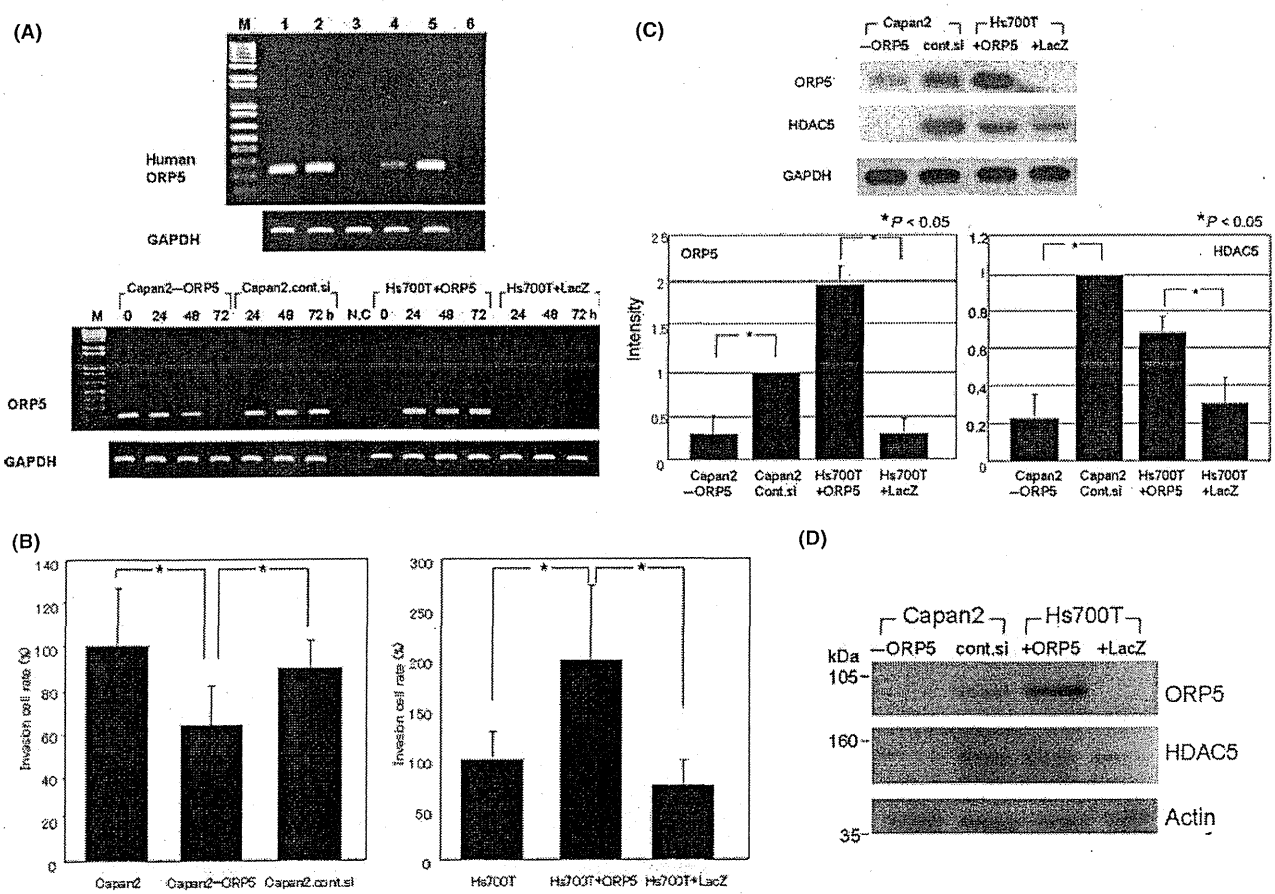

Fig. 1. Suppression and induction of oxysterol binding protein-related protein (ORP) 5 in human pancreatic cancer cell lines. (A) Top, RT-PCR of *ORP5* expression in human pancreatic cancer cell lines. Lane 1, Capan1; 2, Capan2; 3, Hs700T; 4, MiaPaCa2; 5, Panc1; 6, negative control. M, marker. Bottom, RT-PCR of *ORP5* suppression by siRNA in Capan2 (Capan2 – ORP5), and *ORP5* induction by expression plasmid in Hs700T (Hs700T + ORP5). Capan2 cont.si, control siRNA-transfected Capan2; Hs700T + LacZ, LacZ-transfected Hs700T. (B) Invasion assay of *ORP5* suppression and *ORP5* induction. $*P < 0.005$. (C) Regulation of histone deacetylase 5 (HDAC5) by *ORP5*. Top, RT-PCR of ORP5 and HDAC5. Bottom left, intensity of the bands of ORP5 calculated by ImageJ software. Bottom right, intensity of the bands of HDAC5 calculated by ImageJ. $*P < 0.05$. (D) Western blot of *ORP5* and *HDAC5* in the same samples as (C).

doi: 10.1111/j.1349-7006.2009.01475.x

Hs700T as a weakly expressing cell line for future study. *ORP5* suppression of Capan2 by siRNA was observed from 24 h after transfection and maintained for at least 72 h. In Hs700T, *ORP5* induction was observed 24 h after transfection (Fig. 1A). The result of the invasion assay of Capan2 – ORP5 and Hs700T + ORP5 is shown in Figure 1(B). *ORP5* suppression significantly reduced the invasion rate in Capan2 ($P < 0.005$) and *ORP5* induction significantly induced the invasion rate in Hs700T ($P < 0.005$). A cDNA microarray analysis of these samples and the genes suppressed by *ORP5* suppression and induced by *ORP5* induction are shown in Table 2. HDAC5 was suppressed by *ORP5* suppression and induced by *ORP5* induction at both mRNA and protein levels (Fig. 1C,D).

Relation between *ORP5* and cholesterol synthesis. The expression of SREBP2 was examined in Capan2 – ORP5 and Hs700T + ORP5. SREBP2 mRNA expression was reduced in Capan2 – ORP5 and induced in Hs700T + ORP5 (Fig. 2A,B). Additionally, HMG-CoA reductase, which is also an SREBP2 downstream gene, showed the same expression pattern in these cells (data not shown). These results indicate that when *ORP5* is continuously expressed, cholesterol synthesis is commonly stimulated and this might lead to pancreatic cancer invasion. The question therefore remains, how is this pathway involved in cancer invasion and how is it related to *HDAC5* expression?

Table 2. Genes induced by ORP5 expression and also reduced by ORP5 suppression

Gene	GenBank	Product
HDAC4	NM_006037	Histone deacetylase 4
HDAC5	NM_005474	Histone deacetylase 5
TGFB1	NM_000660	Transforming growth factor, beta 1
TGFB3	NM_003239	Transforming growth factor, beta 3
TGFBR3	NM_003243	Transforming growth factor, beta receptor III
ITGA5	NM_002205	Integrin beta 1 isoform 1A precursor
ITGB5	NM_002213	Integrin, beta 5
MDR1	NM_000927	ATP-binding cassette sub-family B member 1

***HDAC5* is the downstream gene of SREBP2.** When the cholesterol synthesis pathway is commonly stimulated, the SREBP2 downstream gene should be expressed. The promoter region of *HDAC5* was examined. Three putative SRE regions were detected within 6 kb of the HDAC5 promoter region (Fig. 2C). A ChIP assay was carried out using Capan2 cells and Hs700T cells. One site was detected within these three putative SREs in Capan2 but not in Hs700T (Fig. 2C).

Expression of *ORP5* after treatment with simvastatin. The effect of statins in pancreatic cancer has been reported.[17] Therefore, the expression levels of *SREBP2* and *HDAC5* were evaluated after treatment with simvastatin. As expected, *SREBP2* and *HDAC5* were suppressed in a dose- and time-dependent manner (Fig. 3A). The invasion rate and growth were also evaluated. The invasion rate of Capan2 was reduced in a dose-dependent manner after 24 h treatment with statins (Fig. 3B). Interestingly, the growth inhibition effect of statins seems to depend on the *ORP5* expression level. In Capan2 and Panc1 (high expression level of *ORP5*), the growth suppression was observed in a dose-dependent manner and required 5 μM statins to suppress the growth to 50%. In MiaPaCa2, which has a moderate *ORP5* expression, only 2.5 μM statins was required to reduce the cell growth to <10%. In Hs700T, which has very weak *ORP5* expression, no growth suppression was observed until 7.5 μM statins was used (Fig. 3C). Similar results were observed in the lovostatin-treated cell lines (Fig. 3D). The growth suppression was weak in Capan2 – ORP5 compared to

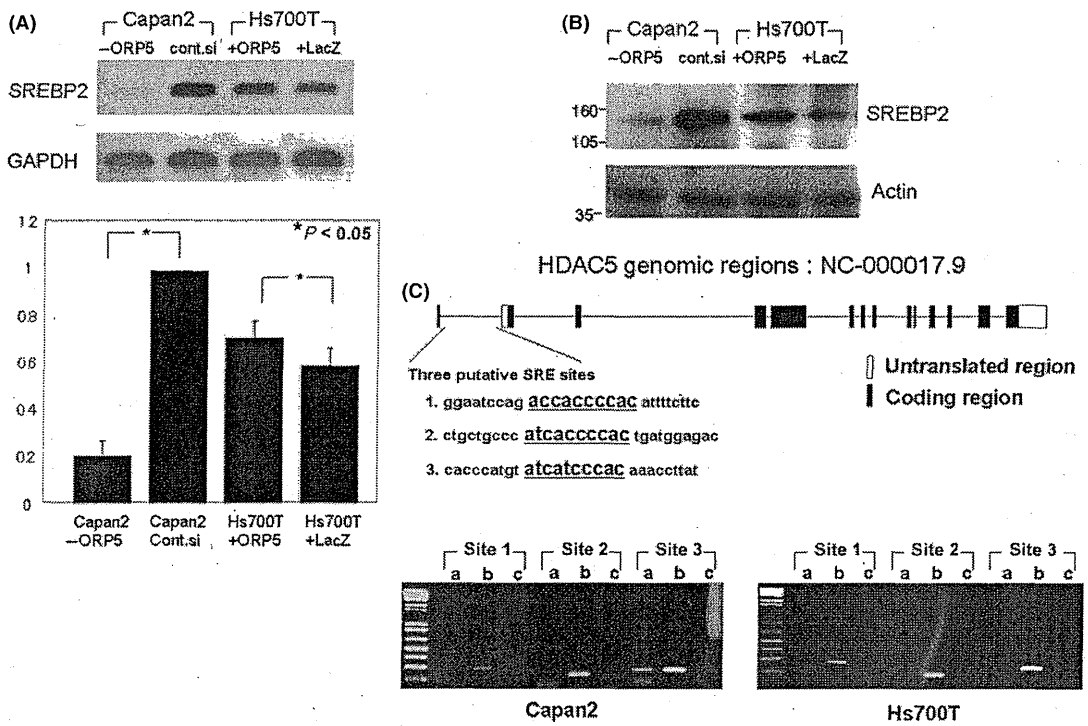

Fig. 2. (A) Regulation of sterol response element binding protein (SREBP2) by oxysterol binding protein-related protein (ORP5). Top, RT-PCR of SREBP2 in *ORP5* suppression an induction. Bottom, intensity of the bands of SREBP2 calculated by ImageJ software. *$P < 0.05$. (B) Western blot analysis of the same sample. (C) ChIP of putative sterol response element (SRE) site in histone deacetylase 5 (HDAC5) genomic region. Top, schematic drawing of the putative SRE site in HDAC5 genomic region. Bottom, results of the ChIP assay of three putative SRE sites. a, ChIP sample; b, input sample (positive control); c, mouse IgG (negative control).

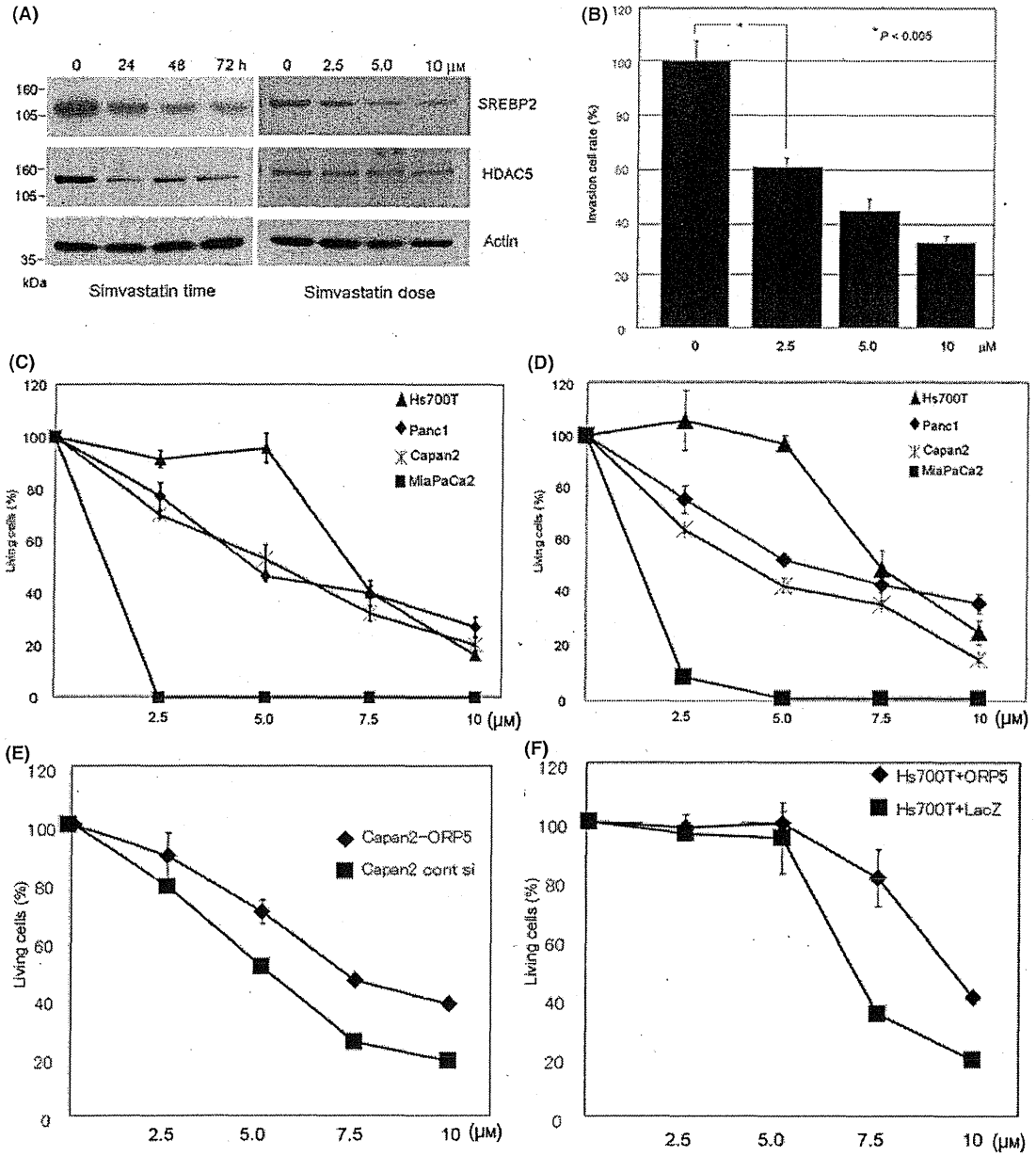

Fig. 3. Effect of statins in pancreatic cancer cell lines. (A) Western blot analysis of sterol response element binding protein (SREBP2) and histone deacetylase 5 (HDAC5) in Capan2 cells treated with simvastatin. Left, after 24, 48, and 72 h of treatment with 5 μM simvastatin. Right, after 48 h of treatment with 2.5, 5.0, or 10 μM simvastatin. (B) Invasion assay of simvastatin-treated Capan2. *$P < 0.005$ (C) Growth assay of pancreatic cancer cell lines treated with simvastatin. (D) Growth assay of pancreatic cancer cell lines treated with lovostatin. (E) Growth assay of ORP5-suppressed Capan2 (Capan2 – ORP5) and control siRNA-transfected Capan2 (Capan2 cont.si) cells treated with simvastatin. (F) Growth assay of ORP5-induced Hs700T (Hs700T + ORP5) and LacZ-transfected Hs700T (Hs700T + LacZ) cells treated with simvastatin.

Capan2 cont.si (Fig. 3E; $P < 0.05$) and when *ORP5* was introduced to Hs700T (Fig. 3F; $P < 0.05$).

Effect of HDAC inhibitor TSA. The invasion and growth assay was carried out using TSA. The invasion rate was significantly reduced at 100 ng/mL TSA (Fig. 4A). Growth inhibition was observed in a dose-dependent manner in Capan2 and Panc1, with strong antitumor effects observed against Hs700T (Fig. 4B). TSA can induce the expression of *PTEN*,[18] thus *PTEN* expression was evaluated after TSA treatment. TSA treatment slightly induced *PTEN* expression in Capan2. The induction of *PTEN* was also observed with *ORP5* suppression and simvastatin treatment (Fig. 4C).

Synergistic growth suppression effect of statin and TSA. Although statins and HDAC inhibitor have tumor suppressive effects, high doses of these drugs are required to suppress growth efficiently. In Capan2, 10 μM simvastatin and 10 μM lovastatin suppressed growth to 20% and 10%, respectively. For TSA, 200 ng/mL would thus be required to suppress the growth to <10%. Therefore, statin and TSA might have a synergistic effect, as these drugs eventually block the same signal transduction. The IC_{50} of simvastatin against Capan2 was 5 μM, and that of TSA was 80 ng/mL, so the dose for each drug was determined as described in 'Materials and Methods'. Interestingly, there was no synergistic effect on invasion (Fig. 5A), however,

doi: 10.1111/j.1349-7006.2009.01475.x

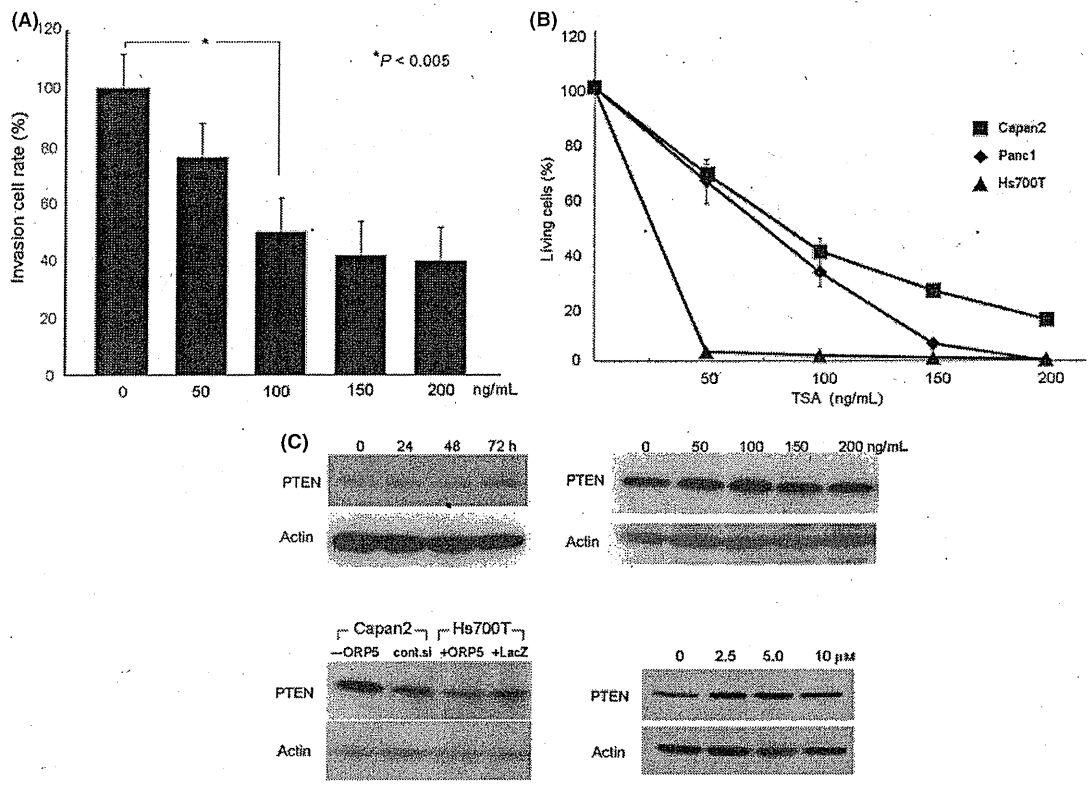

Fig. 4. Effect of trichostatin A (TSA) in pancreatic cancer cell line. (A) Invasion assay of TSA-treated Capan2 cells. *$P < 0.005$. (B) Growth assay of TSA-treated Capan2 cells. (C) PTEN expression in pancreatic cancer cell line. Top, PTEN expression of TSA-treated Capan2 cells (left, 0, 24, 48, and 72 h after treatment with 100 ng/mL TSA; right, 72 h after treatment with 0, 50, 100, 150, or 200 ng/mL TSA). Bottom, PTEN expression of ORP5 suppression and induction (left) and 48 h after treatment with 0, 2.5, 5.0, or 10 μM simvastatin (right). Capan2 cont.si, control siRNA-transfected Capan2; Capan2 – ORP5, ORP5-suppressed Capan2; Hs700T + LacZ, LacZ-transfected Hs700T; Hs700T + ORP5, ORP5-induced Hs700T.

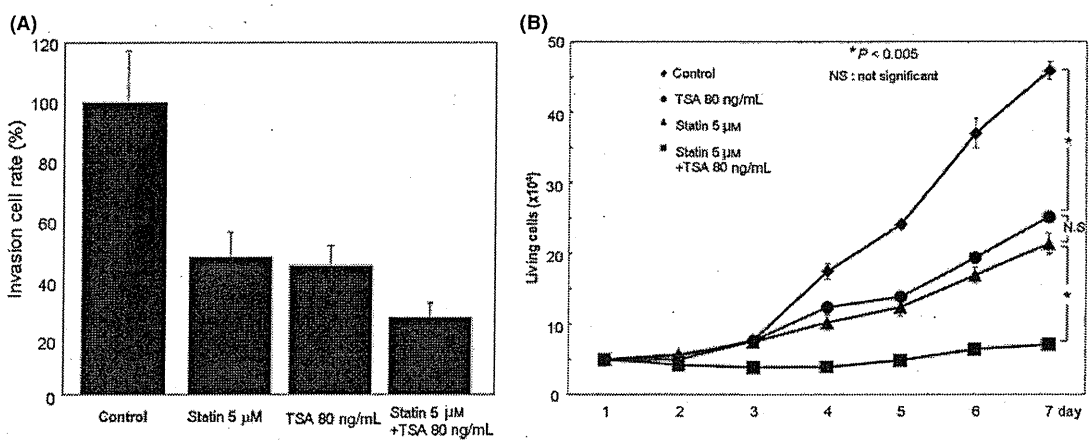

Fig. 5. Synergistic effect of statin and trichostatin A (TSA) in pancreatic cancer cell line. (A) Invasion assay of simvastatin alone, TSA alone, and in combination. (B) Growth assay of simvastatin alone, TSA alone, and in combination. N.S., not significant. *$P < 0.005$.

combination therapy suppressed the growth of Capan2 to <15% (Fig. 5B).

Discussion

The current study revealed several novel findings. First, *ORP5* stimulates the cholesterol synthesis pathway. For some reason, some pancreatic cancer cells express *ORP5*. This gain of function in pancreatic cancer blocks the function of oxysterol and stimulates the cholesterol synthesis pathway. A previous study evaluated several normal human tissues for the expression of *ORP5* using immunohistochemistry. Hepatocytes showed strong *ORP5* expression, and without doubt, liver is the primary organ for cholesterol synthesis.[7] However, this strong expression of *ORP5* in the liver means that targeting *ORP5* directly is impossible for cancer

therapy as it might lead to a severe liver dysfunction. Therefore, the current study focused on the genes downstream of *ORP5*.

Second, cDNA microarray and ChIP assays indicated that *HDAC5* was one of these downstream genes. The result suggests that there is an SRE binding site in the *HDAC5* promoter region and the binding of SRE to the promoter is detected when *ORP5* is continuously expressed. However, the direct target of *HDAC5* is not clear. Pan *et al.* reported that the HDAC inhibitor TSA induces *PTEN* expression by stimulating *Egr1* in the 293T cell line.[18] But this was not observed in pancreatic cancer cell lines. When *ORP5* was suppressed by siRNA, *Egr1* was also suppressed and *PTEN* was induced. This phenomenon was also observed when statins were added to the cell line (data not shown). There must be a different mechanism in pancreatic cancer cell lines. Further study is therefore necessary to clear this pathway.

Third, the effect of statins seems to be regulated by the expression level of *ORP5*. Kusama *et al.* reported that statins reduce invasion and metastasis of human pancreatic cancer.[17] There are arguments that the effect of statins might depend on the status of the *K-ras* mutation.[19] Within the cell lines that were examined in the current study, Capan2, Panc1, and MiaPaCa2 carry a *K-ras* mutation in codon 12 (GGT to TGT, GGT to GAT, and GGT to GTT, respectively) and wild-type is found in Hs700T. The effect of statins was very strong against MiaPaCa2, which has moderate *ORP5* expression. Their effects were dose-dependent in Capan2 and Panc1, which have strong *ORP5* expression, and no effect was found at low doses in Hs700T. This result suggested that when *ORP5* is strongly expressed, the cholesterol synthesis pathway is always stimulated and these cell lines require a high dose of statin to block it. When *ORP5* expression is moderate, only a low dose of statin is necessary. It is not clear why more than 7.5 μM statins was required to suppress the growth of Hs700T, but more than this dose might be simply toxic for this cell line. There is an interesting report concerning the sensitivity of a fibroblast cell line to statins. In this report, when 5 μM statins, which is a clinically available dose, were added to the human lung fibroblast cell line, it induced apoptosis.[20] A normal human fibroblast cell line (Hs68) was examined to confirm this report. This cell line was sensitive to statins from a dose of 2.5 μM, consistent with the report. In addition, this cell line expressed *ORP5* at almost the same level as MiaPaCa2 (data not shown). Furthermore, as this cell line is a normal human fibroblast, no *K-ras* mutation was detected. In our current study, Capan2 – ORP5 became more resistant to simvastatin than Capan2 cont.si. Hs700T + ORP5 also became more resistant to simvastatin than Hs700T + LacZ. These results suggest that when siRNA effectively suppresses *ORP5* in Capan2, these cells lose their sensitivity to statins, and when *ORP5* is introduced to Hs700T, as this transfected plasmid is regulated by a CMV promoter,[7] a strong expression of *ORP5* will occur in the transfected cells and, as a result, Hs700T becomes resistant to statins. These results suggest that when the growth of the cells is dependent on the cholesterol synthesis pathway, it will be sensitive to statins, and the *ORP5* expression level can be the indicator. Although statins are widely used as cholesterol lowering drugs, high doses of statins might be toxic to normal cells and to avoid an unwanted side-effect such as acute hepatitis, the dose should be limited. However, as approximately 60% of pancreatic cancer expresses *ORP5*,[7] a high dose of statins might be necessary to provide a long survival benefit for these patients, even though their serum cholesterol level is low. Which means that statin alone is not sufficient for pancreatic cancer therapy.

Finally, synergistic growth inhibition was observed with the combination of statin and TSA. HDAC inhibitor is a new anticancer reagent and several clinical trials are ongoing. As the dose of HDAC inhibitor for pancreatic cancer patients is not established, clinicians must be careful to avoid side-effects. TSA had a strong antitumor effect against Hs700T (Fig. 4B). Hs700T has weak *HDAC5* expression compared to Capan2 (Fig. 1), thus suggesting that a different mechanism exists for *HDAC5* expression. However, as the expression of *HDAC5* is weak, the antitumor effect by TSA was observed to be in a low density. García-Morales *et al.* reported that TSA induces *p21* and leads to apoptosis in a pancreatic cancer cell line.[21] Donadelli *et al.* showed the synergistic growth suppression of pancreatic adenocarcinoma cell by TSA and gemcitabine.[22] In addition, Bocci *et al.* reported that statin synergistically enhances the antiproliferative effect of gemcitabine in MiaPaCa2.[23] In the current study, a combination of a low dose of statin and TSA had a strong growth inhibitory effect. Although it is unclear why there was no synergistic effect on invasion, these data suggest that a combination of statin and HDAC inhibitor can be a useful and safe anticancer therapy for pancreatic cancers that express *ORP5*.

Recently, Teresi *et al.* reported a relationship between the cholesterol synthesis pathway and *PTEN* expression. This report indicated that statins and SREBP1 induce peroxisome proliferator-activated receptor γ, and this binds directly to the *PTEN* promoter and upregulates *PTEN* mRNA expression in a breast cancer cell line.[24] This report supports the current results. They concluded that both statins and SREBP1 can regulate PTEN transcription, but there must be a different pathway to reach peroxisome proliferator-activated receptor γ. If the cholesterol synthesis pathway is related to breast cancer, statins should lower the risk of breast cancer. Interestingly, although statins can reduce the risk of pancreatic cancer,[25] this is not found in breast cancer.[26,27] Unfortunately, there is no data concerning *ORP5* expression or the relationship between the cholesterol synthesis pathway and the invasion and/or growth of breast cancer, thus the difference in the effect of statins between pancreatic cancer and breast cancer is unknown. However, at least *in vitro*, it seems that there is a relationship between lipid metabolism and tumor suppressor gene expression in both pancreatic and breast cancer cells. Future study might solve this problem.

This is the first report to detail the mechanism by which the cholesterol synthesis pathway is related to cancer invasion and growth. When *ORP5* is expressed in pancreatic cancer, there is a possibility that statins and HDAC inhibitor can provide a useful therapy. Although there are still unknown mechanisms to be cleared, based on this *in vitro* study, *in vivo* experiments as well as a clinical study of combined therapy must be done.

Acknowledgment

This study was supported by a Grant-in-aid from the Ministry of Education, Culture, and Science of Japan.

References

1 Fryzek JP, Garabrant DH, Schenk M, Kinnard M, Greenson JK, Sarkar FH. The association between selected risk factors for pancreatic cancer and the expression of p53 and K-ras codon 12 mutations. *Int J Gastrointest Cancer* 2006; **37**: 139–45.

2 Salek C, Benesova L, Minarik M *et al.* Evaluation of clinical relevance of examining K-ras, p16 and p53 mutations along with allelic losses at 9p and 18q in EUS-guided fine needle aspiration samples of patients with chronic pancreatitis and pancreatic cancer. *World J Gastroenterol* 2007; **13**: 3714–20.

3 Kwon S, Munroe X, Kim YS *et al.* Expression of connective tissue growth factor in pancreatic cancer cell lines. *Int J Oncol* 2007; **31**: 693–703.

doi: 10.1111/j.1349-7006.2009.01475.x

4 Mortenson MM, Galante JG, Bold RJ *et al.* BCL-2 functions as an activator of the AKT signaling pathway in pancreatic cancer. *J Cell Biochem* 2007; **102**: 1171–9.
5 Hirota M, Egami H, Pour PM *et al.* Production of scatter factor-like activity by a nitrosamine-induced pancreatic cancer cell line. *Carcinogenesis* 1993; **14**: 259–64.
6 Ishikawa S, Egami H, Ogawa M *et al.* Identification of genes related to invasion and metastasis in pancreatic cancer by cDNA representational difference analysis. *J Exp Clin Cancer Res* 2003; **22**: 299–306.
7 Koga Y, Ishikawa S, Baba H *et al.* ORP5(oxysterol binding protein related protein 5) is related to invasion and poor prognosis in pancreatic cancer. *Cancer Sci* 2008; **99**: 2387–94.
8 Jaworski CJ, Moreira E, Li A, Lee R, Rodriguez IR. A family of 12 human genes containing oxysterol-binding domains. *Genomics* 2001; **78**: 185–96.
9 Loilome W, Yongvanit P, Wongkham C *et al.* Altered gene expression in Opisthorchis viverrini-associated cholangiocarcinoma in hamster model. *Mol Carcinog* 2006; **45**: 279–87.
10 Fournier MV, Guimarães da Costa F, Paschoal ME, Ronco LV, Carvalho MG, Pardee AB. Identification of a gene encoding a human oxysterol-binding protein-homologue: a potential general molecular marker for blood dissemination of solid tumors. *Cancer Res* 1999; **59**: 3748–53.
11 Rajavashisth TB, Taylor AK, Andalibi A, Svenson KL, Lusis AJ. Identification of a zinc finger protein that binds to the sterol regulatory element. *Science* 1989; **245**: 640–3.
12 Bengoechea MT, Ericsson J. SREBP in signal transduction: cholesterol metabolism and beyond. *Curr Opin Cell Biol* 2007; **19**: 215–22.
13 Inoue J, Sato R, Maeda M. Multiple DNA elements for sterol regulatory element-binding protein and NF-Y are responsible for sterol-regulated transcription of the genes for human 3-hydroxy-3-methylglutaryl coenzyme A synthase and squalene synthase. *J Biochem* 1998; **123**: 1191–8.
14 Raghow R, Yellaturu C, Deng X, Park EA, Elam MB. SREBPs: the crossroads of physiological and pathological lipid homeostasis. *Trends Endocrinol Metab* 2008; **19**: 65–73.
15 Sato R, Inoue J, Kawabe Y, Kodama T, Takano T, Maeda M. Sterol-dependent transcriptional regulation of sterol regulatory element-binding protein-2. *J Biol Chem* 1996; **271**: 26461–4.
16 Schoonjans K, Brendel C, Mangelsdorf D, Auwerx J. Sterols and gene expression: control of affluence. *Biochim Biophys Acta* 2000; **1529**: 114–25.
17 Kusama T, Mukai M, Nakamura H *et al.* Inhibition of epidermal growth factor-induced RhoA translocation and invasion of human pancreatic cancer cells by 3-hydroxy-3-methylglutaryl-coenzyme a reductase inhibitors. *Cancer Res* 2001; **61**: 4885–91.
18 Pan L, Lu J, Huang B *et al.* Histone deacetylase inhibitor trichostatin a potentiates doxorubicin-induced apoptosis by up-regulating PTEN expression. *Cancer* 2007; **109**: 1676–88.
19 Müller C, Bockhorn AG, Koch OM *et al.* Lovastatin inhibits proliferation of pancreatic cancer cell lines with mutant as well as with wild-type K-ras oncogene but has different effects on protein phosphorylation and induction of apoptosis. *Int J Oncol* 1998; **12**: 717–23.
20 Tan A, Levrey H, Dahm C, Polunovsky VA, Rubins J, Bitterman PB. Lovastatin induces fibroblast apoptosis in vitro and in vivo. A possible therapy for fibroproliferative disorders. *Am J Respir Crit Care Med* 1999; **159**: 220–7.
21 García-Morales P, Gómez-Martínez A, Saceda M *et al.* Histone deacetylase inhibitors induced caspase-independent apoptosis in human pancreatic adenocarcinoma cell lines. *Mol Cancer Ther* 2005; **4**: 1222–30.
22 Donadelli M, Costanzo C, Palmieri M *et al.* Synergistic inhibition of pancreatic adenocarcinoma cell growth by trichostatin A and gemcitabine. *Biochim Biophys Acta* 2007; **73**: 1095–106.
23 Bocci G, Fioravanti A, Danesi R *et al.* Fluvastatin synergistically enhances the antiproliferative effect of gemcitabine in human pancreatic cancer MIAPaCa-2 cells. *Br J Cancer* 2005; **93**: 319–30.
24 Teresi RE, Planchon SM, Waite KA, Eng C. Regulation of the PTEN promoter by statins and SREBP. *Hum Mol Genet* 2008; **17**: 919–28.
25 Khurana V, Sheth A, Caldito G, Barkin JS. Statins reduce the risk of pancreatic cancer in humans: a case-control study of half a million veterans. *Pancreas* 2007; **34**: 260–5.
26 Kuoppala J, Lamminpää A, Pukkala E. Statins and cancer: a systematic review and meta-analysis. *Eur J Cancer* 2008; **44**: 2122–32.
27 Pocobelli G, Newcomb PA, Trentham-Dietz A, Titus-Ernstoff L, Hampton JM, Egan KM. Statin use and risk of breast cancer. *Cancer* 2008; **112**: 27–33.

Supporting Information

Additional Supporting Information may be found in the online version of this article:

Table S1. List of genes examined by cDNA microarray.

Please note: Wiley-Blackwell are not responsible for the content or functionality of any supporting materials supplied by the authors. Any queries (other than missing material) should be directed to the corresponding author for the article.

Int J Clin Oncol (2010) 15:39–45
DOI 10.1007/s10147-009-0008-2

ORIGINAL ARTICLE

Clinical significance of dihydropyrimidine dehydrogenase and thymidylate synthase expression in patients with pancreatic cancer

Osamu Nakahara · Hiroshi Takamori · Hiroshi Tanaka · Yasuo Sakamoto · Yoshiaki Ikuta · Satoshi Furuhashi · Masayuki Watanabe · Toru Beppu · Masahiko Hirota · Keiichiro Kanemitsu · Hideo Baba

Received: 2 December 2008 / Accepted: 29 June 2009 / Published online: 14 January 2010

Abstract
Background Little is known about the clinical significance of TS and DPD in pancreatic cancer. We aimed to evaluate TS and DPD expression levels in not only pancreatic cancer but also surrounding normal pancreatic tissues to assess the clinical implications of the expression of TS and DPD in this study.
Patients and methods Pancreatic cancer and normal pancreatic tissues were obtained from 18 patients with pancreatic cancer who underwent pancreatic resection to measure TS and DPD activities. The TS and DPD activities were determined by enzyme-linked immunosorbent assay using non-fixed fresh-frozen specimens.
Results Pancreatic cancer tissues had significantly higher DPD and TS enzyme activities than surrounding normal tissue. Anaplastic ductal carcinoma had higher DPD and TS activities than the other histological types. Patients with high DPD in this study demonstrated poorer prognosis than those with low DPD. On the other hand, there was no statistically significant difference in survival between the high and the low TS groups.
Conclusions The efficacy of 5-FU may be lower in pancreatic cancer tissue than in normal tissue because DPD activity is upregulated in pancreatic cancer tissue compared to normal pancreatic tissue. It is necessary to develop an effective 5-FU delivery system and/or 5-FU combined with an inhibitor for DPD that can be used when 5-FU must be administered to patients with pancreatic cancer. High DPD activity may be a prognostic factor in patients with pancreatic cancer.

Keywords Pancreatic cancer · Dihydropyrimidine dehydrogenase · Thymidylate synthase

O. Nakahara · H. Takamori · H. Tanaka · Y. Sakamoto · Y. Ikuta · S. Furuhashi · M. Watanabe · T. Beppu · M. Hirota · K. Kanemitsu · H. Baba (✉)
Department of Gastroenterological Surgery,
Graduate School of Medical Sciences, Kumamoto University,
1-1-1 Honjo, Kumamoto 860-8556, Japan
e-mail: hdobaba@kumamoto-u.ac.jp

Introduction

Pancreatic cancer has increased in incidence over the past several decades [1], and still remains a lethal disease, because the annual incidence of it has been shown to be approximately equal to the annual death rate caused by it [2]. The overall 5-year survival rate is below 5% in all patients with pancreatic cancer [3]. Despite improvements in imaging technology, fewer than 20% cases are potentially resectable at the time of initial diagnosis [4]. Most patients are suffering from a systemic disease at the time of diagnosis. Surgical resection offers the only chance for cure, but even after curative resection there is a high probability of systemic and/or local relapses [5–7]. Therefore, surgery alone is clearly an inadequate approach to achieve long-term survival in patients with respectable pancreatic cancer. 5-Fluorouracil (5-FU) is widely used in the treatment of gastrointestinal tumors, including pancreatic cancer. Thymidylate synthase (TS) is an important enzyme for DNA synthesis and the target for 5-FU. Previous clinical studies have demonstrated that TS expression level predicts the response to 5-FU-based chemotherapy [8–10]. Moreover, patients with node-positive breast cancer with high TS expression demonstrated the most significant benefit of adjuvant 5-FU-containing chemotherapy. Dihydropyrimidine dehydrogenase (DPD) is the rate-limiting enzyme for 5-FU catabolism. Moreover, several

clinical studies have revealed that DPD expression in cancer tissues is associated with 5-FU resistance and poor outcomes [11–13]. Reported data on TS and DPD activities in pancreatic cancer are limited, and little is known about the significance of TS and DPD activities in patients with pancreatic cancer.

We aimed to evaluate the expression levels of TS and DPD in not only pancreatic cancer tissues but also surrounding normal pancreatic tissues, and assess the clinical significance of the expression of TS and DPD in this study.

Patients and methods

Clinical samples

Between October 2002 and December 2005, surgical specimens were obtained from 18 patients with pancreatic cancer who underwent pancreatic resection at Kumamoto University. Written informed consent was obtained from each patient before the treatment. Tumor and normal pancreatic tissues were collected from resected specimens to measure TS and DPD activities. All samples were immediately frozen at −80°C until use. According to the classification of pancreatic cancer defined by the Japanese Pancreas Society [14], we evaluated histological characteristics including tumor location, histological stage and histological classification.

Reagents

5-FU was purchased from Wako Pure Chemicals (Tokyo, Japan). [6-^{14}C]-5-FU (56 mCi/mmol) was obtained from American Radiolabeled Chemicals Inc. (St. Louis, MO, USA) and [6-^{3}H] FdUMP (16.9 Ci/mmol) from Moravek Biochemicals Inc. (Brea, CA, USA). All other chemicals used were commercial products of the highest quality available.

Enzyme assay

Approximately 200 mg of the frozen tissue were homogenized with 4 v of 50 mM Tris–HCl (pH 7.6) containing 10 mM 2-mercaptoethanol, 25 mM KCl, and 5 mM $MgCl_2$, and after centrifuging at 105,000×g for 60 min, the supernatant was taken to measure the TS and DPD activities. TS was measured by the [6-^{3}H]-FdUMP binding assay based on the method of Spears et al. [15]. DPD was assayed by a modified form of the method of Nagplate Naguib et al. [16], as described previously [17]. Briefly, a reaction mixture containing 10 mM potassium phosphate (pH 8.0), 0.5 mM EDTA, 0.5 mM 2-mercaptoethanol, 2 mM dithiothreitol, 5 mM $MgCl_2$, 20 μM [6-^{14}C]-5-FU, 0.1 mM NADPH, and 25 μl of enzyme extract in a total volume of 50 μl was determined as the sum of the products formed from 5-FU: dihydrofluorouracil (DHFU), 2-fluoro-β-ureidopropionic acid, and 2-fluoro-β-alanine. After adding 25 μl of 0.36 mM KOH, the reaction mixture was allowed to stand at room temperature for at least 30 min to hydrolyze the DHFU formed, and it was then neutralized with 25 μl of 0.36 mM $HClO_4$ and immediately centrifuged at 14,000 rpm for 10 min. A 5 μl aliquot of the supernatant was applied to a silica gel $60F_{254}$ plate (2.5 × 20 cm, Merck, Darmstadt, Germany) and developed with a mixture of methanol and 1 M ammonium acetate (5:1, v/v). Each product was visualized and quantified with an imaging analyzer (BAS-2000, Fujix, Tokyo, Japan).

Statistical analysis

We used Student's t test to compare the TS and DPD activities of tumor tissue and normal pancreatic tissues. The cumulative survival curve in this series was depicted using the Kaplan–Meier method, and levels of significance were tested using the log-rank test. Differences were considered to be statistically significant at $p < 0.05$.

Results

Patient characteristics

The patients' characteristics are summarized in Table 1. The study subjects included 8 females and 10 males. The median age of the patients was 61 years, and ranged from 48 to 76 years. The primary pancreatic lesion was located in the head in 11 patients, in the body in 5, and in the tail in 2. Of the 18 patients in total, 16 received 5-FU administration pre- and/or postoperatively. We performed radical operations and 13 of the patients underwent intraoperative radiation therapy. Histological differentiation was good in 9, moderate in 5, poor in 2, and anaplastic carcinoma in 2. Of the 18 patients, 16 were affected by stage IV disease.

DPD and TS activity in pancreatic cancer and normal tissues

DPD activity was successfully measured in 18 samples of tumor tissues and 12 of normal tissues. DPD activity was revealed to be significantly higher in tumor tissues (395.3 ± 51.8) than in surrounding normal tissues (178.6 ± 15.08) (Fig. 1). TS activity was successfully measured. Measurable TS activity was also significantly higher in tumor tissue (0.028 ± 0.0068) than in

surrounding normal tissue (0.009 ± 0.0048) (Fig. 2). According to the histological classification, DPD activity was 349.00 ± 30.43 in well-differentiated types, 410.17 ± 177.50 in moderately differentiated types, 334.41 and 353.65 (mean = 344.03) in poorly differentiated types, and 634.80 and 600.85 (mean = 617.83) in anaplastic ductal carcinomas. Anaplastic ductal carcinoma was the highest level of DPD in tumor tissue (Fig. 3). The TS activity level was 0.018 ± 0.004 in the well-differentiated type, 0.026 ± 0.005 in the moderately differentiated type, 0.035 and 0.042 (mean = 0.039) in the poorly differentiated type, and 0.028 and 0.11 (mean = 0.069) in anaplastic ductal carcinoma. TS activity was higher in anaplastic ductal carcinoma than in the well-differentiated type (Fig. 4). There was no correlation between DPD and TS activities (correlation coefficient = 0.320, $p = 0.21$). Moreover, there was no significant difference in DPD and TS activities among clinicopathological features, including age, sex, site of primary lesion, histological stage, and serum marker (Table 2).

Table 1 Patient characteristics

No. of patients	18
Age (years)	
Median	61
Range	48–76
Male/female	10/8
Site of primary lesion	
Ph	11
Pb	5
Pt	2
Pancreatectomy	
PD + IORT	1
PpPD (+IORT)	8
DP (+IORT)	8
SSPpD + IORT	1
Histological stage	
III	2
IVa	10
IVb	6
Histological classification	
Well-diff. tub.	9
Mod. diff. tub.	5
Poorly diff. tub.	2
Anaplastic carcinoma	2

PD pancreaticoduodenectomy
PpPD pylorus preserving pancreaticoduodenectomy
DP distal pancreatectomy
SSPpD subtotal stomach-preserving pancreaticoduodenectomy
IORT intraoperative radiation therapy

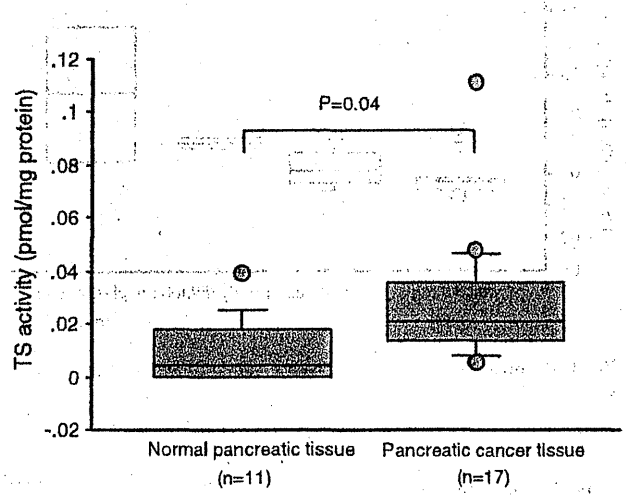

Fig. 2 Comparison of TS activity between pancreatic cancer and normal pancreatic tissues

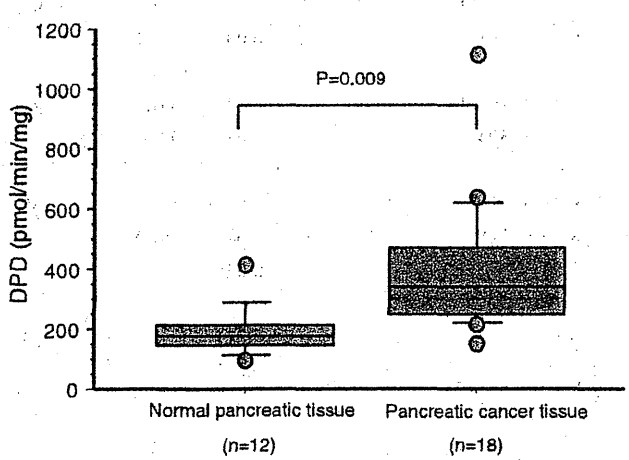

Fig. 1 Comparison of DPD activity between pancreatic cancer and normal pancreatic tissues

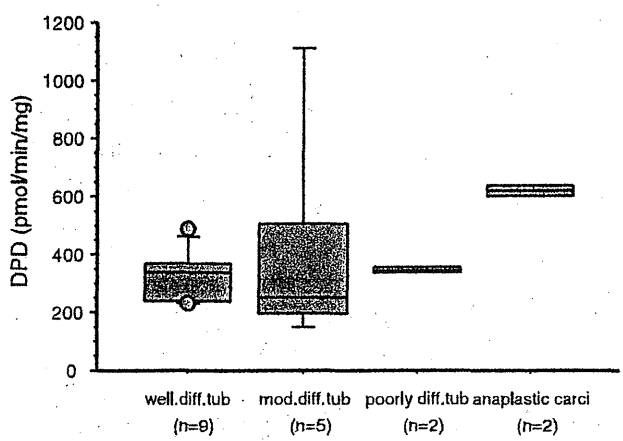

Fig. 3 Comparison of DPD activity according to histological classification

Survival

We categorized the patients into high- and low-activity groups using the mean levels of DPD and TS in the cancer tissues as cutoff thresholds. The prognosis of patients in the high DPD activity group was poorer than that of the patients in the low DPD activity group. The mean dose of 5-FU administered per patient was 8.75 g in the high DPD group and 14.6 g in the low DPD activity group. There was no statistically significant difference in the total doses of 5-FU of the two groups. The high-DPD activity group had a poorer prognosis than the low-DPD group (Fig. 5), although there was no statistically significant difference in the clinical features of the two groups (Table 3). There was also no statistically significant difference in survival between the high- and the low-TS activity groups (Fig. 6).

Discussion

The expression of DPD and TS in pancreatic cancer tissues has been shown using several methods, including germline polymorphisms, mRNA levels, and immunohistochemistry [18–20]. As far as we know, this is the first report of the

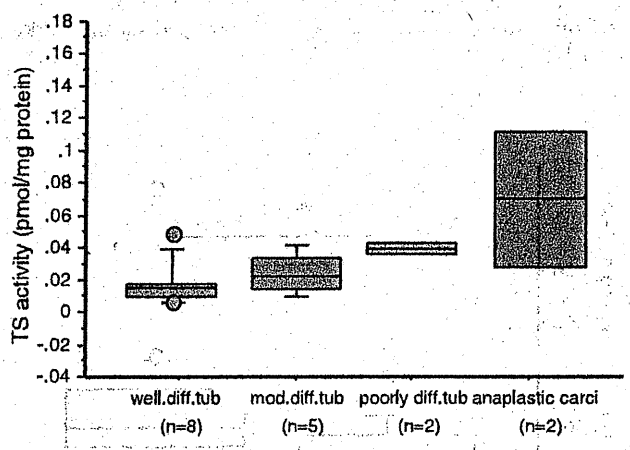

Fig. 4 Comparison of TS activity according to histological classification

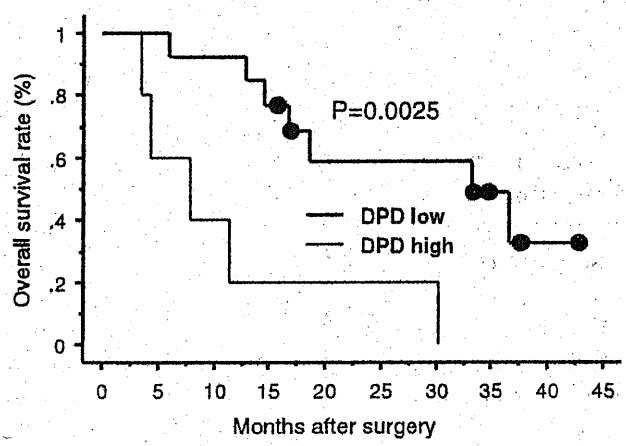

Fig. 5 Comparison between the high and the low DPD activity groups

Table 2 Correlation between clinicopathological features and DPD and TS activities

Variables	Number of patients (n = 18)	DPD activity	P value	TS activity	P value
Age					
<60	8	337.70 ± 85.89	0.46	0.024 ± 0.018	0.592
≥60	10	419.02 ± 291.93		0.031 ± 0.030	
Sex					
Male	10	318.41 ± 109.28	0.178	0.022 ± 0.013	0.338
Female	8	463.47 ± 304.03		0.034 ± 0.034	
Site of primary lesion					
Ph	11	299.91 ± 91.60	0.11	0.023 ± 0.015	0.469
Pb	5	548.30 ± 348.77		0.042 ± 0.047	
Pt	2	425.68		0.025	
Histological stage					
III	2	358.16	0.084	0.011	0.183
IVa	10	291.58 ± 97.01		0.022 ± 0.014	
IVb	6	543.28 ± 321.77		0.043 ± 0.035	
Serum marker					
Responders	14	336.72 ± 125.06	0.281	0.028 ± 0.030	0.926
Nonresponders	4	478.41 ± 427.66		0.027 ± 0.013	